CRHyME (Climatic Rainfall Hydrogeological Model Experiment): a new model for geo-hydrological hazard assessment at the basin scale

Andrea Abbate[1], Leonardo Mancusi[1], Antonella Frigerio[1], Monica Papini[2], Laura Longoni[2]

[1]RSE, Ricerca Sistema Energetico, Via Rubattino 54, Milano
5 [2]Politecnico di Milano, Piazza Leonardo da Vinci 32, Milano

Correspondence to: Andrea Abbate (andrea.abbate@rse-web.it)

Abstract. This work presents the new model called CRHyME (Climatic Rainfall Hydrogeological Modelling Experiment), a tool for the geo-hydrological hazard evaluation. CRHyME is a physically based and spatially distributed model written in Python language and represents an extension of the classic hydrological models that simulate inflows-outflows at the basin
10 scale. A series of routines have been integrated to describe the phenomena of geo-hydrological instabilities such as the triggering of shallow landslides as well as debris flows, catchment erosion, and sediment transport into the river. These phenomena are generally decoupled with respect to the continuous hydrological simulation while in CRHyME they are quantitatively and simultaneously evaluated through a multi-hazard approach.

CRHyME has been tested on some case studies located in Italian basins. Valtellina and Emilia's areas were considered for the
15 calibration and validation procedures of the model thanks also to the availability of literature data concerning past occurred geo-hydrological instability phenomena. Calibration and validation of the model conducted on presented case studies have been assessed through some hydrological indexes such as NSE (Nash–Sutcliffe Efficiency) and RMSE (Root Mean Square Error) while for landslide phenomena the ROC (Receiver Operating Characteristic) methodology was applied. CHRyME has been able to: 1) reconstruct the surface runoff at the reference hydrometric stations located at the outlets of the basins, 2)
20 estimate the solid transport at some hydropower reservoirs compared to the reference data, and 3) evaluate the triggering of shallow landslides and debris flows compared to those recorded in the literature. The ranking has shown a rather good performance of the model in terms of numerical conservativity of water and solid balances, revealing suitable not only for back-analysis studies but also as an efficient tool for Civil Protection multi-hazard assessment.

1 Introduction

25 Landslides, floods, and debris flows represent serious geo-hydrological hazards in mountain environments (Gariano and Guzzetti, 2016). Shallow landslides and debris flows are often the result of soil erosion and sediment transport (Brambilla et al., 2020; Papini et al., 2017; Longoni et al., 2016; Ballio et al., 2010) and they can build up over long timescales due to the intermittency of mass wasting processes controlled by rainfall triggering events of varying intensity and duration (Abbate et al., 2021a). Natural disasters are a critical problem both in terms of economic losses and causalities (ISPRA, 2018). Only in

30 2020, the worldwide losses related to geohazard were quantified as 210 billion dollars and 8'200 victims (Munich Re, 2021).
Among the natural disasters, the events linked to geo-hydrological phenomena, such as floods and landslides, certainly play a
significant role. In Italy, a total area of 50'117 km2, which corresponds to 16.6% of the national territory is affected by high
or very high landslide hazards and/or by a medium hydraulic hazard (ISPRA, 2018). In 2021, the victims of landslide and
flood events were five and the evacuated people were around 1'000 (CNR and IRPI, 2021). Northern Italy has the highest

35 mortality rate caused by landslides and floods (number of deaths and missing people per 100'000 people in one year) in the
country, varying in the range of 0.034 for Emilia Romagna and 0.085 for Piedmont.

Geo-hydrological hazards are complex and heterogeneous phenomena, so a great deal of effort has been made in the past to
try and interpret their dynamics and triggering factors (Gariano and Guzzetti, 2016; Ceriani et al., 1994; Gao et al., 2018; Kim
et al., 2020). There are many studies concerning shallow landslide dynamics in the literature-based both on laboratory and

40 field experiments (Guzzetti et al., 2007; Herrera, 2019; Meisina et al., 2013; Crosta et al., 2003; Iverson, 2000; Ivanov et al.,
2020b), which individuate rainfall as the main triggering factor for this type of phenomenon. However, in the literature is still
missing a widely accepted methodology that can connect strongly the different components that have an interplay role in geo-
hydrological hazards generation and evolution (Gariano and Guzzetti, 2016; Bordoni et al., 2015). In this context, shallow
landslides, debris flow and solid transport are primarily driven by superficial soil water balance that can also influence the

45 runoff generation through the infiltration mechanisms (Abbate et al., 2019).

In this work the potentiality of a new physically-based geo-hydrological model called CRHyME is illustrated. CRHyME is an
extension of a classical rainfall-runoff hydrological model where also geo-morphological dynamic aspects are taken into
account. From the analysis of the literature (De Vita et al., 2018; Bemporad et al., 1997; Roo et al., 1996; Schellekens et al.,
2020; Angeli et al., 1998; Gleick, 1989; Sutanudjaja et al., 2018; Van Der Knijff et al., 2010; Devia et al., 2015; Moges et al.,

50 2021), rarely the two aspects have been jointly analysed. A lot of hydrological models, adopted worldwide, are interested
mainly in flood propagation and water balance assessment (Sutanudjaja et al., 2018). One of their main limitations is that they
are rather advanced in the hydrological part, proposing a very detailed description of the hydrological cycle while geo-
hydrological hazards interaction is barely taken into account (Shobe et al., 2017; Strauch et al., 2018). Up to now, there are
still few examples that can include the triggering analysis of shallow landslide and debris flow, or a solid transport

55 quantification (Roo et al., 1996; Gariano and Guzzetti, 2016; Alvioli et al., 2018). In literature, some examples consider the
erosion and solid transport mechanisms at the watershed scale (Vetsch et al., 2018; Tangi et al., 2019; Roo et al., 1996; Papini
et al., 2017) while the stability of natural slopes is still not properly included in distributed hydrological models and vice-versa.
The stability of slopes or debris flow analysis is computed inside dedicated models such as (Iverson, 2000; Scheidl and
Rickenmann, 2011; Harp et al., 2006; Milledge et al., 2014; Montrasio, 2008; Takahashi, 2009) that takes into account some

60 aspect of the hydrological cycle but they are not fully integrated into a rainfall-runoff routine. Moreover, several models have
limiting spectra of application mainly due to several limitations such as input data requirements, the scale of simulation, data
resolution and simulated processes (Devia et al., 2015; Moges et al., 2021).

In this regard, CHASM (Combined Hydrology and Stability Model) (Bozzolan et al., 2020) and Landlab (Strauch et al., 2018) represent the two latest modelling frameworks that have addressed the need to start evaluating the geo-hydrological hazard and risks considering also hydrological and climatical aspects. The new methodological approaches shown by CHASM and Landlab models have been assessed thanks to the progressively increasing data availability for GIS (Geographical Information Systems) on a worldwide scale and thanks to the recent improvements in computer programming for environmental systems. Indeed, the creation of efficient and open-source built-in functions for different language programs, such as Matlab, C++ or Python, has sped up and facilitated the implementation of self-made earth-surface models. This is the case of PCRaster libraries (Karssenberg et al., 2010) that have been written in Python language. The PCRaster Python framework offers a series of standard functions prepared for hydrological processing on calculation grids that schematize a territory. Functions can be easily "called" via scripts in Python to perform individual computational operations, which allows for building new models, as in the case of CRHyME. These function libraries have been already successfully implemented by PCR-GLOBWB-2 (Sutanudjaja et al., 2018) and WFLOW (Schellekens et al., 2020) models, as well as in the European hydrological model LISFLOOD (Van Der Knijff et al., 2010) and OPENLISEM (Roo et al., 1996).

Starting from these considerations and taking inspiration from these models, the first version of CRHyME was developed. This paper presents the main features of the CRHyME model. Structure and constitutive equations are reported in the Material and Method section. Then the case studies are taken into account for the calibration and validation procedure of the new model. In the Result sections the main outcomes of CRHyME applications are reported and they are extensively commented on in the Discussion and Conclusions sections.

2 Material and Methods

This paragraph presents the CRHyME model (Figure 1), created for a correct quantification of the hazard deriving from floods and landslides at basin scale.

2.1 Model novelties

CRHyME's engine is based on PCRaster libraries (Karssenberg et al., 2010; Pebesma et al., 2007) which is a collection of open-source software targeted at the development and deployment of spatio-temporal environmental models. These functions can include a rich set of model building blocks and analytical functions for manipulating raster GIS maps, a framework for the construction of stochastic spatio-temporal models and a tool for interactive visualisation of spatio-temporal data. They are mainly applied in environmental modelling such as rainfall-runoff models and slope stability models and can deal with spatially distributed earth surface data that are discretized considering the single cell of terrain domain as the reference element where model calculations are carried out. Using PCRaster libraries, 4 different processes that describe quantitatively the geo-hydrological hazards that may occur at the catchment scale have been implemented:

- River flow discharge and volume;
95 - River erosion and sediment transport discharge and volume;
- Shallow landslide triggering condition;
- Debris flow triggering condition.

The most innovative part of the code includes the physical relations that describe how the hydrological assessment can influence and potentially trigger the geo-hydrological hazards occurring at the basin scale:

100 - The sediment transport in terms of the bed-load process has been described considering the Erosion Potential Method (EPM) (Longoni et al., 2016; Brambilla et al., 2020; Milanesi et al., 2015; Ivanov et al., 2020a) for simulating erosion processes and the stream power laws available in the literature for defining the transport capacity of the rivers (Vetsch et al., 2018).

- For shallow landslide modelling, slope stability models commonly adopted in engineering geology have been
105 implemented to evaluate the stability conditions of natural slopes (Iverson, 2000; Montrasio, 2008; Harp et al., 2006; Milledge et al., 2014). The selection of the stability model depends on the number and type of landslides (e.g., deep-seated, shallow), the type and amount of information available to characterize the slope or landslide, and the extent of the study area (e.g., a single slope or landslide, a catchment, a large geographical region). In CRHyME, we were interested mainly in the simulation of the shallow landslide.

110 - According to (Theule, 2012; Jakob and Jordan, 2001), defining a rigid boundary between flood, solid transport, debris flow and shallow landslide processes is not always possible. Debris flows phenomena reside in the middle so defining a unique criterion for analysing their instability cannot be assessed straightforwardly since they can behave intermediately among floods and landslides. Following the theory proposed by (Takahashi, 2009), debris flows triggering infinite-slope-like criteria were adopted considering also a second condition that includes information on
115 the river flow discharge.

The aim was to merge the potentiality of the reference models cited before : including a well-organized model framework, already adapted to work with meteorological reanalysis and climate scenarios data (PCR-GLOBWB-2), predicting and quantifying some geo-hydrological processes (Landlab and CHASM), and extending the event-based simulation (OPENLISEM) to a continuous simulation over a longer period.

120
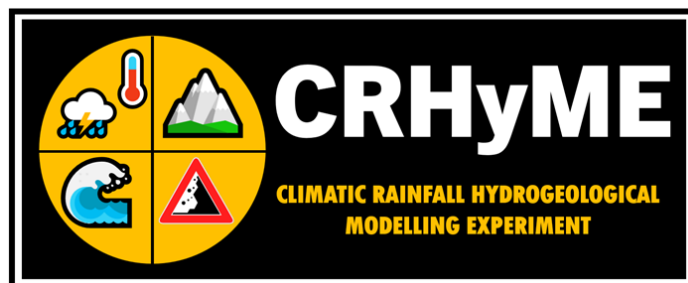
Figure 1: CRHyME logo.

2.2 Model Structure

125 The CRHyME model is composed of a series of modules connected in a time-loop as represented in Figure 2. The simulations
are initialized from a pre-compiled .INI file (see the appendix A) where all the settings and input data paths are specified (see
the Appendix B). In the .INI file are essentially reported the simulation time settings (e.g. starting date and ending date), the
spatially distributed input data and the meteorological and climatological data series, the settings of each computational module
and the name of the output files. The .INI file is read by the "deterministic_runner.py" file that starts the CRHyME model and
130 its internal routines. Except for "pre-processing.py", "reporting.py" and "plot.py" modules, where variables are respectively
defined, saved, and plotted following the formats and standards of the PCRaster libraries (Sutanudjaja et al., 2018; Karssenberg
et al., 2010), other modules contain the physical equations that aim to simulate the geo-hydrological cycle.

1. CLIMA: elaborates precipitation and temperature data from climate datasets, using the "NetCDF" (Network
   Common Data Form) format (Bonanno et al., 2019; Sutanudjaja et al., 2018);

135 2. METEO: elaborates precipitation and temperature data from ground-bases weather stations using the PCRaster
   standard format ".tss" (Karssenberg et al., 2010) for data series and calculates the evapotranspiration;

3. INTERCEPTION + SNOW: excludes from net precipitation the canopy interception and the snow;

4. LANDSURFACE: evaluates the water balance in the superficial soil giving information about runoff, soil
   moisture and percolation losses;

140 5. GROUNDWATER: evaluates the water balance in the groundwater layer;

6. ROUTING: calculates the runoff routing across the watershed;

7. LANDSLIDE: identifies the triggering conditions for landslides, and debris flows and calculates erosion and
   bed-load sediment transport in rivers.

The first 6 modules constitute the "hydrological modules" and are deputed for assessing the hydrological cycle while the
145 "landslide module" individuates slope instability conditions and simulates sediment transport considering the computed soil
moisture and runoff.

Figure 2: **Framework and modules of the model CRHyME.**

150   The PCRaster libraries implemented in CRHyME have the advantages to be fully parallelized to work with multicore processors (Karssenberg et al., 2010). This is an important aspect of our code that permits us to decrease sharply the time-consuming of each simulation. The intrinsic parallelization of the PCRaster libraries is embedded in the PCRaster functions so that the code can be written directly without any further parallelization optimizations. In Table 1 some estimations of the operating time calculation ranked for the model CRHyME are reported.

155

	PCRaster N° Workers	Single Operation with a large file (10'000 cells)	Single Cycle of model Iteration
2 cores	2	4.07 s	Around 20 – 25 s
4 cores	4	1.48 s	Around 8 – 10 s
8 cores	8	1.05 s	Around 5 – 6 s

Table 1: Performances of CRHyME model working on different CPU core sets. It can be noticed that by increasing the number of cores available, the computation time for a particular operation can drop significantly.

2.2.1 Input spatial data

160

The digital terrain model used in CRHyME as a starting point for the computations is provided by HydroSHEDS (Hydrological data and maps based on SHuttle Elevation Derivatives at multiple Scales) (Lehner et al., 2008). It represents a hydrologically conditioned elevation raster at 3-sec degree resolution which corresponds approximately to about 90 m at the equator. This digital elevation model (DEM or DTM) is designed to be used in hydrological models (Lehner et al., 2008): the model has

165 been already pre-processed to guarantee the flowing connectivity of the river network, which is required to make consistent and fasters the hydrological computations. Its nominal resolution of 90 m at the equator is considered sufficient for the evaluation of slope parameters for soil stability analysis at the catchment scale but in principle, CRHyME can work with any spatial resolutions.

Starting from the HydroSHEDS DTM, and using the PCRaster functions (Karssenberg et al., 2010; Pebesma et al., 2007) is

170 possible to automatically generate data on the territorial morphology, such as the directions of the maximum slope and the reconstruction of the hydrographic network. Moreover, slope and aspects can be automatically generated from DTM.

In addition to these morphology data other layers required in the CRHyME model for the geo-hydrological assessment are:

- the Corine Land Cover data (https://land.copernicus.eu) (Girard et al., 2018);
- the soil texture data at 250 m resolution obtainable from the world database ISRIC — World Soil Information

175 (https://maps.isric.org/) (Hengl et al., 2017);

- the hydraulic properties of soils, such as the permeability, the maximum terrain water content and porosity, are available from the European database (https://esdac.jrc.ec.europa.eu/) and other worldwide repositories (Tóth et al., 2017; Ross et al., 2018; Huscroft et al., 2018);

The layer listed in Figure 3 are available freely for the entire European area, but similar data can be found for other continents

180 and worldwide countries. Since they are provided with an open-source licence they can be implemented without restrictions. Using the GDAL libraries for Python (GDAL/OGR contributors, 2020), the geographical data has been converted to the PCRaster standard format ".map" for raster data (Karssenberg et al., 2010; Sutanudjaja et al., 2018), considering WGS84 datum as a reference system for geographical projection. An automatic procedure that allows extracting all the required territorial data at the catchment scale has been built up in Python to facilitate the elaborations. It connects directly to WFS and

185 WCS services of the cited databases downloading the data required. It will be included in the future version of the model as a CRHyME pre-processor.
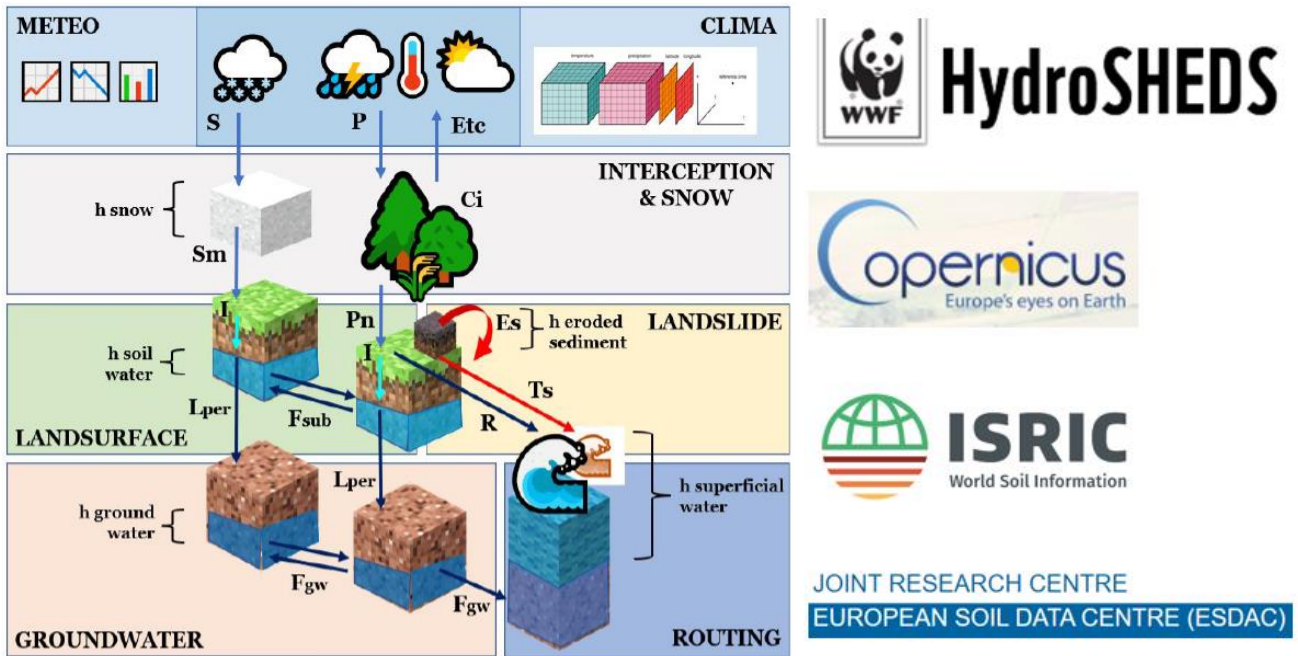
190 **Figure 3:** Scheme of the terrain water-balance model and fluxes in CRHyME and input datasets.

2.2.2 Hydrological module and equations

The "hydrological modules" (from 1 to 6) evaluate the processes of transformation inflows-outflows using input maps of weather forcings consisting of precipitation $[mm\ timestep^{-1}]$ and average, maximum, and minimum temperature $[C^\circ]$. The model also calculates evapotranspiration losses $ETc(t)$ according to two formulations chosen by the user: Hargreaves and

195 Pennman-Montheit, both taken from FAO guidelines (Raziei and Pereira, 2013; Allan et al., 1998). Although during intense precipitation events the evapotranspiration portion can often be neglected (Chow et al., 1988), its calculation is essential for continuous long-term hydrological simulations. Moreover, this is important also for short-term simulations because may influence the initial conditions of the soil moisture $S_m(t)$ (Abbate et al., 2019; Lazzari et al., 2018; Mostbauer et al., 2018).

The hydrological part of CRHyME follows a standard implementation, where each cell of the terrain domain is considered as

200 a tank that communicates in cascade to the others (Brambilla et al., 2020; Roo et al., 1996; Sutanudjaja et al., 2018) following the downstream river network. The hydrological cycle that normally takes place in the first 2 m of soil layers is described considering the interaction of the rainfall with the surface through the canopy interception, infiltration, and percolation processes and also snow accumulation and melting are simulated. The superficial terrain soil moisture evolution and the runoff generation are assessed at each time step across the catchment domain. In CRHyME the runoff routing is computed

205 considering the kinematic approach (Chow et al., 1988).

Hydrological balance is schematized considering 4 imaginary layers where water can be temporally stored:

1. Snow Storage, Eq. (1) where snow balance assessed by $\mathrm{h}_{snow}(\mathrm{t})$ variable, $[mm]$,

2. Superficial Soil Storage, Eq. (2) and (3) where infiltration is computed and superficial soil balance is assessed by $\mathrm{h}_{soilwater}(\mathrm{t})$ variable, $[mm]$,

3. Groundwater Soil Storage, Eq. (4) where groundwater balance is assessed by $\mathrm{h}_{groundwater}(\mathrm{t})$ variable, $[mm]$,

4. Runoff Storage, Eq. (5) where runoff generated by an excess of infiltration and exfiltration is routed across the catchment and described by the quantity $\mathrm{h}_{runoff}(\mathrm{t})$, $[mm]$.

Superficial soil is schematized by Eq. (2) and Eq. (3) and the fluxes in this layer are evaluated $[mm\ timestep^{-1}]$:

- Canopy Interceptions $C_I(t)$: that is the part of the rainfall intercepted by trees leaves;
- Snowmelt $S_{ml}(t)$ and Snow $S(t)$: the melted snow coming from the snowpack;
- Infiltration $I(t)$: that is the part of the volume that enters the soil using two of the most common infiltration models Horton and SCS-CN (Chow et al., 1988; Chen and Young, 2006; Mishra et al., 2003; Morbidelli et al., 2018; Ravi et al., 1998; Smith and Parlange, 1978; Ross et al., 2018);
- $L_{per}(t)$ losses: e.g. the part of the volume that goes to the deepest layer, evaluated as a function of the soil water balance in unsaturated conditions using Van Genucten's functions and parameters (Jie et al., 2016; Van Genuchten, 1980; Daly et al., 2017; Groenendyk et al., 2015; Vitvar et al., 2002; Jackson et al., 2014; Klaus and Jackson, 2018);
- Exfiltration $Ex(t)$ and $Ex_{GW}(t)$: e.g. the leakage of water on the surface (groundwater) following the complete saturation of the soil (aquifer) column.
- $F_{sub}(t)$ and $F_{GW}(t)$: lateral fluxes generated inside superficial soil layer and groundwater layer, following the Dupuit law for unsaturated – saturated soils.
- $F_{kin-dyn}(t)$: runoff fluxes computed using the kinematic or dynamic flow routing PCRaster functions.

All the fluxes related to water mass balance are converted to the standard international units such as $[m^3 s^{-1}]$ for discharges while storage quantities $\Delta\mathrm{h}_{snow}(\mathrm{t}), \Delta\mathrm{h}_{soilwater}(\mathrm{t}), \Delta\mathrm{h}_{groundwater}(\mathrm{t})$ and $\Delta\mathrm{h}_{runoff}(\mathrm{t})$ are converted into $[m^3]$ for volumes. $S_m(t)$ is expressed in $[mm]$ and converted to adimensional quantity $[-]$ if divided by product of the terrain porosity n and height.

$$\frac{dh_{snow}(t)}{dt} \cong \frac{\Delta\mathrm{h}_{snow}(\mathrm{t})}{\Delta\mathrm{t}} = \mathrm{S}(\mathrm{t}) - \mathrm{S}_{ml}(\mathrm{t})$$	(1)

$$I(t) = P(t) - C_I(t) - S_{ml}(t) - R(t) = P_n(t) - R(t)$$	(2)
$$S_m(t) = \frac{dh_{soilwater}(t)}{dt} \cong \frac{\Delta\mathrm{h}_{soilwater}(\mathrm{t})}{\Delta\mathrm{t}} = \mathrm{I}(\mathrm{t}) - \mathrm{ETc}(\mathrm{t}) - \mathrm{Ex}(\mathrm{t}) - \mathrm{L}_{per}(\mathrm{t}) \pm \mathrm{F}_{sub}(\mathrm{t})$$	(3)

$$\frac{dh_{groundwater}(t)}{dt} \cong \frac{\Delta h_{groundwater}(t)}{\Delta t} = L_{per}(t) - Ex_{GW}(t) \pm F_{GW}(t) \qquad (4)$$

$$\frac{dh_{runoff}(t)}{dt} \cong \frac{\Delta h_{runoff}(t)}{\Delta t} = R(t) + Ex(t) + Ex_{GW}(t) \pm F_{kin-dyn}(t) \qquad (5)$$

235

At the groundwater reservoir, the sub-surface flow is generated thanks to the percolated water from the upper layer Eq. (4). The flow is calculated using the Dupuit approximation according to which the filtration rate is given by the product of hydraulic permeability for the tangent of the slope of the impermeable substrate, supposed parallel to the slope (Klaus and Jackson, 2018; Anderson, 2005; Bresciani et al., 2014). The sub-surface flow has been modelled considering a special distribution of the

240 groundwater depth (Fan et al., 2007; de Graaf et al., 2015; Pelletier et al., 2016). This approximation has appeared sufficiently precise concerning the fact that up to now available data on groundwater aquifer depth and hydrogeology parameters are rather approximated and uncertain with respect to the affordability of the superficial layers data (Kobierska et al., 2015; Zomlot et al., 2015; Hayashi, 2020; Huscroft et al., 2018).

The sum of the surface and the emerged sub-surface runoffs are propagated along the lines of maximum slope and the river

245 network using two possible methods available in PCRaster libraries that are deputed for the flow routing process (Chow et al., 1988; Lee and Pin Chun, 2012; Collischonn et al., 2017; Bancheri et al., 2020): kinematic and dynamic. Both derive from the simplification of De Saint Venant's one-dimensional equations of motion. The first is generally used in sections where the slopes are accentuated so it is possible to approximate the hydraulic gradient with the slope of the channel (Chow et al., 1988). The second instead introduces further terms that allow a better simulation of the outflow in correspondence to the flat areas

250 where the other terms of the De Saint Venant equation are no longer negligible (Chow et al., 1988), but requires precise information about the geometry of rivers sections to carry out the flood wave propagation.

2.2.3 Geo-hydrological module and equations

In order to study geo-hydrological instability, especially in hilly and mountain areas, it is of paramount importance to analyse the triggering causes of landslides and the dynamic of erosion processes (Guzzetti et al., 2005; Remondo et al., 2005; Montrasio

255 and Valentino, 2016; Bovolo and Bathurst, 2012). For this purpose, in the CRHyME model, a "landslide module" (7) has been developed and tested.

2.2.3.1 Stability models for shallow landslides

Since shallow landslides triggering is strongly correlated with meteorological and climatic forcing (Abbate et al., 2021a), the

260 detection of their possible failure has been implemented in CRHyME model. The abrupt modification of the local hydrology due to the alternation of dry and wet conditions of soil induced by precipitation is responsible for undermining the stability of the slopes (Iverson, 2000; Chen and Young, 2006). In the literature, there are various examples of the application of stability

models for shallow landslides (Abbate et al., 2019; Buma, 2000; Bordoni et al., 2015; Ivanov et al., 2020b). Here are described briefly the four stability models included in CRHyME:

265
1. Iverson model (Iverson, 2000), Eq. (6),
2. Harp model (Harp et al., 2006), Eq (7)
3. Milledge model (Milledge et al., 2014) and, Eq (8)
4. SLIP model (Montrasio, 2008; Montrasio and Valentino, 2016), Eq. (9).

The one-dimensional theory that considers the hypothesis of infinitely extended slope stability is guaranteed by the safety

270
factor (FS) defined as the ratio between the resistant forces compared to the mobilizing ones. The model is based on the concept of limit equilibrium of the inclined plane for which the weight component of the specific gravity γ_s parallel to the slope, having a slope α, is destabilizing while the friction force allows the ground to remain in balance.

$$FS = \frac{\tan(\varphi)}{\tan(\alpha)} - \frac{\psi \gamma_w \tan(\varphi)}{\gamma_s Z \sin(\alpha)\cos(\alpha)} + \frac{c}{\gamma_s Z \sin(\alpha)\cos(\alpha)} \qquad (6)$$

$$FS = \frac{\tan(\varphi)}{\tan(\alpha)} + \frac{m \gamma_w \tan(\varphi)}{\gamma_s \tan(\alpha)} + \frac{c}{\gamma_s Z \sin(\alpha)} \qquad (7)$$

275

$$FS = \frac{2F_{rl} + F_{rb} + F_{rd} - F_{du}}{F_{dc}} \qquad (8)$$

$$FS = \frac{N' \tan\varphi + C'}{W' \sin\alpha + F'} \qquad (9)$$

The key parameters of the Iverson and Harp model are essentially 3:

- The friction angle of the soil φ [°]: is an intrinsic property of the soil that is a function of the grain sorting,
280
- The cohesion of the soil c [kPa]: is an intrinsic property of the soil that is a function of the grain size sorting,
- The water content of the soil is obtained as a ratio between the thickness of soil Z and the height of the aquifer that is locally created at the slope. In Iverson's model is described by the variable ψ which represents the hydraulic load of the local aquifer, expressed in [kPa] while in the Harp model is described by the variable m which is the % of soil moisture with respect to the Z.

285
Milledge model considers not only the friction effects along the sliding surface (F_{rb}), expressed in [N], but also the following parameters:

- The cut resistance along the side walls that have stabilized function, F_{rl}, in [N],

- The passive force of the upstream terrain, which has a destabilizing function F_{du}, in $[N]$,
- The active force of the valley terrain, which has to stabilize function F_{rd}, in $[N]$.

290 In the SLIP model the terms are expressed in $[N]$:

- N' is the normal component of the weight as a function of porosity n, and parameters m and S_m. m is an analogue of Harp model, while S_m, is a corrective parameter depending on the season of the year,
- C' is the cohesion term, also in function of m and S_m,;
- W' is the slope parallel component of the weight as a function of porosity n, and parameters m and S_m,;
295 - F' is the term that expresses the seepage forces that are related to the presence of the temporal water table.

Since watershed-scale slopes are vegetated two other factors should be included: the additional cohesion of the root system of trees and the additional weight of plant biomass (plants). These two parameters proved to be very important, especially for the correct interpretation of the slope dynamics at the vegetated slopes (Cislaghi et al., 2017; Yu et al., 2018; Rahardjo et al., 2014). In fact, in the absence of radical cohesion, those portions were perpetually in conditions of instability with FS < 1. The
300 addition of root cohesion, varying between 1 – 10 kPa depending on the tree species and the type of land use, has made it possible to correct the estimates of the stability model.

In CRHyME, the one-dimensional model was implemented by imagining each cell as a slope element for which the value of the safety factor FS is calculated. Typical values of the friction angle and cohesion for superficial terrains have been obtained from literature references, while the water content is the result of the hydrological balance carried out by hydrological modules.
305 According to the principle of effective stress, as the soil moisture increases, normal efforts are reduced by an aliquot equal to the pressure generated by the water itself (Iverson, 2000). Consequently, when the ground is completely saturated there is a drastic decrease in the friction component and an increase in the weight of the ground both play a penalizing role against the stability of the slope. It is no coincidence that, in nature, surface landslides occur during intense meteorological events in which the water content of the soil undergoes a sudden increase due to both local rain and surface and sub-surface recirculation of
310 water (Abbate et al., 2021a). In this regard, the implementation of the hydrological module in CRHyME has allowed us to leave out the conservative hypothesis about the completely saturated slope that is normally considered precautionary against the assessment of stability (Montgomery and Dietrich, 1994).

2.2.3.2 Stability models for debris flow

315 The debris flow represents an eventually huge movement of mass that can be triggered on steep slopes and travel long distances reaching the fan of the watershed outlet (Takahashi, 2009). They are diffused all over the world and their dynamic depends mainly on the characteristic of the source area that can provide sufficient material for collapse and mobilization (Hungr et al., 2008; Mostbauer et al., 2018; Rickenmann, 1999). The main important controlling parameter of debris flow is the concentration of the soil component (Takahashi, 2009). These type of events set intermediately between shallow landslides, where the solid
320 behaviour is prevalent, and floods where liquid rheology is the driving force (Iverson et al., 1997). Therefore, solid concentration with respect to the water saturation of the source deposit and the presence of superficial water flowing is the key

parameter for assessing the triggering condition. To include this capability for debris flow triggering prediction, in CRHyME the criteria proposed by Takahashi have been taken into consideration. As can be appreciated by the Eq. (10) and (11), two criteria are at least to be included. The first one is derived from the theory of infinite slope stability where the solid

325 concentration parameter C_* is included as the principal triggering factor. C_* is the grain concentration by volume in the static debris bed and can be expressed by the ratio between the soil content $[m^3]$ in respect to the sum of the soil content and soil water volume $[m^3]$. Increasing the local water volume, the soil concentration starts to progressively reduce. The criterium requires the indication of soil density σ $[kgm^{-3}]$, water density ρ $[kgm^{-3}]$, the surface runoff height h $[m]$ and the parameter a that can be assumed equal to the representative diameter of the soil deposit, such as D_{50}, expressed in $[m]$. The second

330 criterium considers that a sufficient superficial runoff q_l above the debris flow deposit is present, expressed in $[m^3 s^{-1}]$.

$$FS_{debris} = \dfrac{\dfrac{C_*(\sigma - \rho)}{C_*(\sigma - \rho) + \rho\left(1 + \dfrac{h}{a}\right)}\tan\varphi}{tan\theta}$$	(10)
$$q_* = q_l / \sqrt{D_{50}{}^3 * g} \geq 2$$	(11)

Debris flow deposits are generally constituted by incoherent material that is cohesionless (Iverson et al., 1997; Takahashi, 2009; Rickenmann, 1999). It doesn't exist a map or a unique criterion to identify their collocation inside a watershed basin

335 even if it is explicitly remarked in the land use map. Therefore, if only the first criterion is applied in all parts of the basin, may all the parts will appear unstable because the cohesion is completely neglected. The second criterion is necessary because can reduce the area affected by debris flow susceptibility. The former has also a physical interpretation since debris flow incoherent deposits may generally accumulate in lateral valley impluvium where are stable is assured by dry conditions (Theule, 2012). When it rains, the impluvium may generate locally a high concentration of runoff fluxes that can destabilise the deposit and

340 generate debris flow.

2.2.2.3 Erosion production and bed-load solid transport evaluation

Gavrilovic's method was initially developed in southern ex-Yugoslavia and then successfully applied also in Switzerland and Italy, it is a semi-quantitative method capable of giving an estimation of erosion and sediment production in a basin (Longoni

345 et al., 2016; Milanesi et al., 2015; Globevnik et al., 2003; Brambilla et al., 2020). Eq. (12) represents the synthesis of Gavrilovic's method. The average annual volume of eroded material G, expressed in $[m^3 yr^{-1}]$, is a product of W_s and R, which are respectively the average annual production of sediment due to surface erosion, expressed in $[m^3 yr^{-1}]$ Eq. (13), and the retention coefficient, adimensional $[-]$ in Eq. (14), which considers the possible re-sedimentation of the eroded material across the watershed.

$$G = W_S R$$	(12)

$$W_s = \pi H \tau_G Z^{\frac{3}{2}} A$$	(13)
$$R = \frac{\sqrt{OD}(l + l_{lat})}{(l + 10)A}$$	(14)

350

The terms that appear in the equations are T temperature coefficient [$°C$], H average annual precipitation value [$mm yr^{-1}$], Z erosion coefficient [$-$], A basin area [km^2], O perimeter of the basin [km], D average height of the basin [km], l length of the main water course [km], l_{lat} the total length of the lateral tributaries [km]. The values of Z are obtained from experimental tables reported in the appendix and are generally correlated to the land use characteristics and geological maps. The Gavrilovic

355 method was developed to work with annual data of mean precipitation and temperature. Since with CRHyME we are interested in a continuous simulation, the method has been temporally downscaled substituting P and T at yearly bases with the time-step precipitation [$mm\ timestep^{-1}$] and temperature [$C°\ timestep^{-1}$].

Gavrilovic method defines W_s as the source of available sediment that can be routed through the watershed until the outlet. In CRHyME the solid routing has been modelled considering its strong relation with liquid discharge. In particular, the solid

360 discharge is calculated in two manners. A first calculation considers a pure Transport Limited bed load transport (Morgan and Nearing, 2011; Shobe et al., 2017; Campforts et al., 2020), where the solid discharge is expressed as a power-law function of the river channel slope and liquid discharge. The latter is corrected by recalling the theory of incipient motion of Shields that states the starting motion of sediments in the function of D_{50} quantity (Chow et al., 1988; Merritt et al., 2003; Vetsch et al., 2018). A second calculation recalls the kinematic model under the strong hypothesis that the velocity of sediment transport,

365 when the critical value of incipient motion has overcome, is assumed like the water flow. Several authors (Govers, 1989; Govers et al., 1990; Rickenmann, 1999) have considered this hypothesis reasonable when no further additional information about solid transport is available.

The first implementation of solid transport routing and balance is founded on the hypothesis of Transport Limited (TL) as a prevalent condition. The second one is rather more representative of the Erosion Limited (EL) condition (Shobe et al., 2017;

370 Campforts et al., 2020) where the material available in the river or on the slopes tends to limit effective water erosion. In both cases, the sediment balance has been assessed considering erosion (E_s), deposition (D_s) and transport term (T_s), with Eq. (15). In CRHyME both TL and EL are evaluated for solid transport assessment. According to (Papini et al., 2017; Ivanov et al., 2020a; Dade and Friend, 1998; Lamb and Venditti, 2016; Peirce et al., 2019; Pearson et al., 2017; Ancey, 2020), the evaluation of the process of sediment transport activation is a research frontier where a complete interpretation of the process has not

375 been acquired yet, Figure 4. Among others, the spatial distribution of D_{50} is the most uncertain parameter that has been found to sharply modify the effective sediment transport routing and the watershed sediment yield in CRHyME. The absence of realistic spatial distribution data about terrain granulometry that are capable to distinguish among slopes and river environments can complicate the effective reproduction of the erosion processes. Recently, some efforts have moved in this

direction (Abeshu et al., 2021; Nino, 2002) but further steps are still needed especially across hilly and mountain environments
380   where complexities arise due to local geology and morphology.
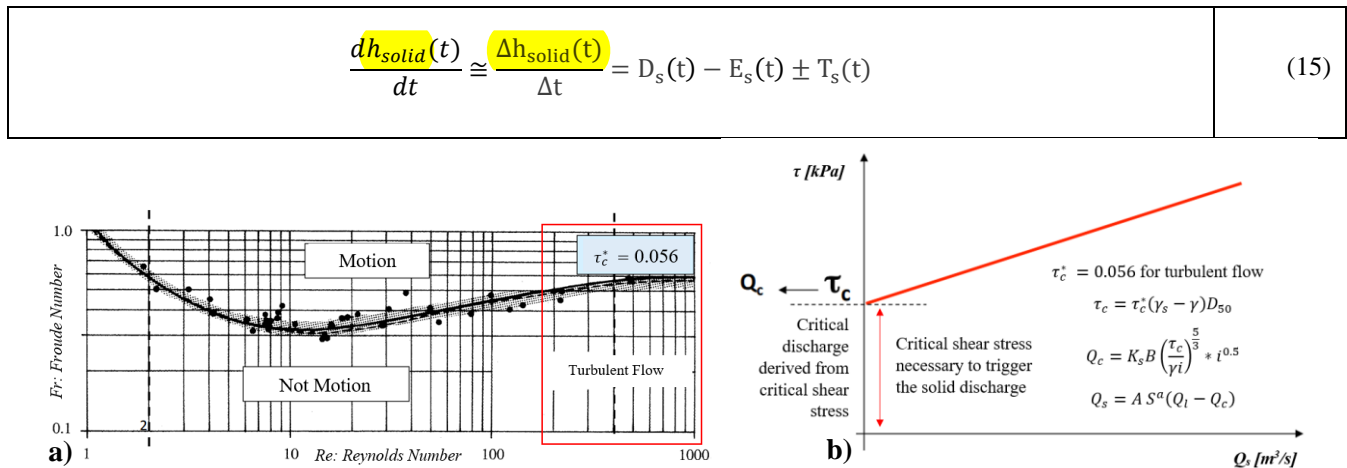
$$\frac{dh_{solid}}{dt}(t) \cong \frac{\Delta h_{solid}(t)}{\Delta t} = D_s(t) - E_s(t) \pm T_s(t)$$	(15)

Figure 4: a) Shield abacus for solid transport incipient motion under different conditions of turbulence (Re number) and flow regime (Fr number). In the red box is defined the typical range of turbulent flow in rivers with a critical adimensional shear stress τ_c^* of
385   **0.056; b) evaluation of the incipient motion condition for solid transport where the critical shear stress τ_c and the critical liquid discharge Q_c are a function of the local granulometry through the parameter D_{50}.**

In the recent literature, some simplified models of sediment erosion and transport have been proposed to fulfil the need to quantify these processes (Tangi et al., 2019; Bizzi et al., 2021; Czuba, 2018; Gilbert and Wilcox, 2020; Beveridge et al., 2020). The models described represent a strong idealization of what can happen at the catchment scale. Some authors have proposed
390   a framework where the river network is discretized in "segments" where the mass balance of water and solid are assessed starting from the top of the basin up to the outlet. These "topological" frameworks are fast and rather simple to interpret and have the peculiarity to include all the infrastructures, such as dams, that can perturb the sediment balance at reached levels (Tangi et al., 2019; Bizzi et al., 2021; Schmitt et al., 2018). One of their main worth points is the possibility to include statistical analysis on inputs and making Montecarlo iterations to reach the best accordance with monitoring field data. Montecarlo
395   statistical technique is applied especially for assessing the granulometry of each reach of the catchment where the sediment source strongly depends on the characteristic diameters (Tangi et al., 2019). In several cases, an automatic procedure has been implemented and rather large catchments have been studied (Bizzi et al., 2021; Schmitt et al., 2018). However, these models suffer from the same problems as the distributed ones: the scarcity of reference data that are necessary to select the more realistic Montecarlo simulation and the not complete understanding of the erosion-transport processes. According to
400   (Beveridge et al., 2020; Sklar et al., 2017), the erosion processes on the hillslopes are rather complex and are difficult to conceptualize in a unique framework since several factors work together at different scales and at different times to manipulate the soil granulometry. In particular, sediment delivery to river reaches depends on landslides that occurred in the past that are a barely random process without a characteristic of periodicity (Gilbert and Wilcox, 2020; Sklar et al., 2017). Moreover, several

assumptions on transport dynamics are assumed in these models such as the hypothesis of equilibrium of the sediment supply
405   across the rivers (Bizzi et al., 2021; Gilbert and Wilcox, 2020) that, in some cases, maybe not be representative of the real
condition that is again barely unknown. Due to their simplicity, these models are generally not integrated with a hydrological
routine because are intended to focus only on sediment transport mechanisms (Bizzi et al., 2021; Gilbert and Wilcox, 2020;
Beveridge et al., 2020). So, liquid discharge data series are required to be initialized and some hypothesis about uniform flow
motion using Gauckler-Manning-Strickler formula are needed to associate a proper discharge value at each river reach.

2.3 Model performance

The CRHyME model is strongly physical-based. During the calibration and validation phase of the CRHyME model, some
benchmarking indicators have been considered both for assessing the performances of hydrological and slope-stability parts
(Bancheri et al., 2020) and they are reported in the next section.

2.3.1 Hydrological Indexes and assessment

415   Assessing hydrological performance at basin outlets is necessary to indirectly understand if the water balance has been
modelled correctly (Chow et al., 1988). Generally, a comparison between water discharges recorded by the local hydrometer
and the water discharge simulated by the model is carried out (Chow et al., 1988; Bancheri et al., 2020). Exist several indexes
that permit retrieving a good-worse model performance from this comparison. The most common are Nash–Sutcliffe
Efficiency (NSE), and Root-Mean-Square Error (RMSE).

420   ▪   The Nash–Sutcliffe Efficiency (NSE) (Eq. 16) is a normalized model efficiency coefficient. It determines the relative
magnitude of the residual variance compared with the measured data variance where S_i and M_i are the predicted and
observed values at a given time step. The NSE varies from −∞ to 1, where 1 corresponds to the maximum agreement
between predicted and observed values.

$$NSE = 1 - \frac{\sum_{i=1}^{n}(S_i - M_i)^2}{\sum_{i=1}^{n}(M_i - \bar{M}_i)^2}$$ (16)

425   ▪   The Root-Mean-Square Error (RMSE) (Eq. 17) is given by where M and S represent the measured and simulated
time series, respectively, and N is the number of components in the series.

$$RMSE = \sqrt{\frac{1}{N}\sum_{i=1}^{n}(M_i - S_i)^2}$$ (17)

For CRHyME validation, we have considered NSE and RMSE as reference indicators both for water discharge comparison
and for the total volume cumulated, retrieved from the temporal integration of the water discharge.

430

2.3.2 Sediment Transport assessment

Up to now, it doesn't exist a methodology or a specific monitoring system that permits an evaluation of the solid transport discharge (Morgan and Nearing, 2011; Milanesi et al., 2015). the bathymetry campaign inside hydropower plants reservoirs can be considered as benchmark data for determining the bedload agreement with the Gavrilovic model evaluations (Pacina et

435 al., 2020; Langland, 2009; Marnezy, 2008). The main drawback of these data is that in some cases are not accessible to the public and can be found only if a specific study or report has been conducted. Fortunately, for the case studies these data were retrieved from specific reports (Milanesi et al., 2015; Ballio et al., 2010) and also acquired through bathymetric campaigns (Brambilla et al., 2020). Therefore, sediment transport was validated considering two data sources: 1. seasonal volume estimation in hydro plants reservoirs, 2. event-based volume estimation found in literature.

440

2.3.3 ROC curves for local landslide prediction

According to several authors (Formetta et al., 2016; Pereira et al., 2016; Vakhshoori and Zare, 2018; Gudiyangada Nachappa et al., 2019; Kadavi et al., 2018; Fawcett, 2006), a useful technique to assess the good prediction of slope stability models is the Receiver Operating Characteristic (ROC) methodology. ROC curve is a graphical plot that illustrates the diagnostic ability

445 of a binary classifier system as its discrimination threshold is varied. In landslide stability assessment, the binary classificatory is the condition of FS > 1 (stable) or FS < 1 (unstable) that each pixel of the model can match in the function of the local morphology (slope), terrain characteristics and hydrological conditions (Formetta et al., 2016; Vakhshoori and Zare, 2018).

The CRHyME model doesn't build a susceptibility map but it simply counts the number of the landslide activation on each timestep if the instability condition of FS < 1 is verified. The spatial scale where the activations are represented is the pixel

450 dimension of the HydroSHED DEM. This resolution may be sufficient to spot a single shallow landslide activation but there are uncertainties on its real extension that could be in principle lower or greater than single-pixel size.

According to (Harp et al., 2006), the inclusion of a "pixel-buffer" in the surrender area of a shallow landslide is necessary to describe more physically the process of shallow landslide activation. Bearing in mind that the single-pixel evaluation may be too reductive, in CRHyME, the activation of a single-pixel considers also a buffer around its 8 cells, as reported Figure 5. This

455 choice has been confirmed by the observation of the existing Italian landslide databases (IFFI: Inventario Fenomeni Franosi Italiano) (ISPRA, 2018) where the typical spatial extension is comprised of between 200^2 m^2 and 400^2 m^2. It seems reasonable that these extensions are a true representation of the geometry of a shallow landslide so that for each activation detected, 9 pixels have been switched on simultaneously.
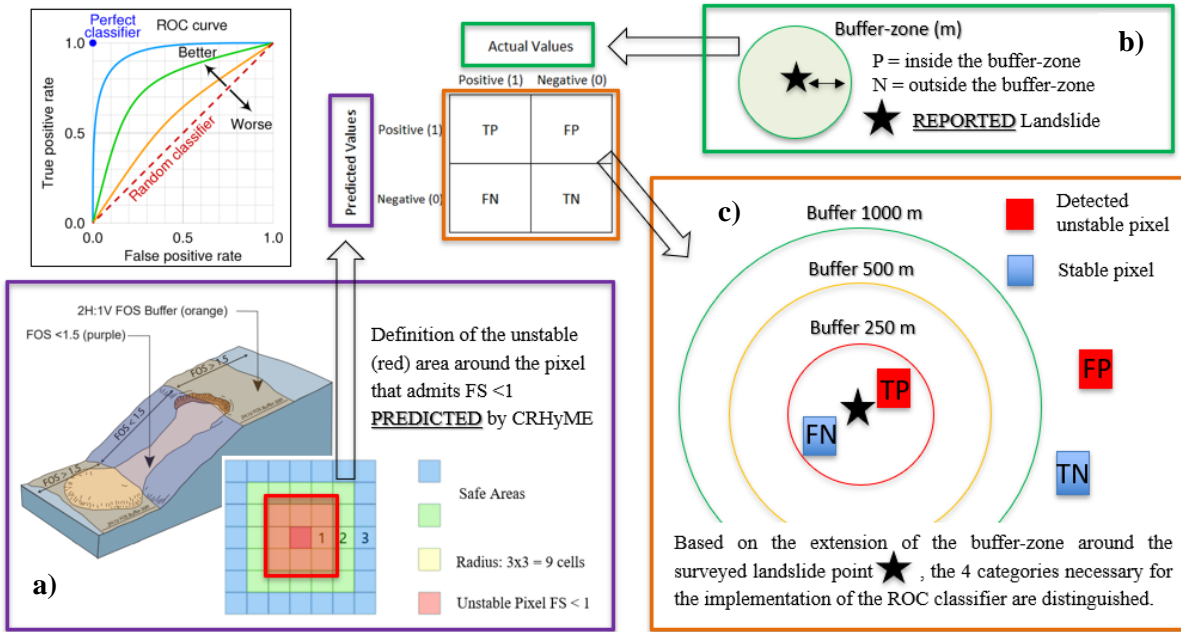
460

Figure 5: a) Extension of unstable pixel computed by model CRHyME considering the surrounded 8 cells, b) buffer-zones defined for each reference landslide point with different extensions and c) workflow of the ROC methodology with the evaluation of parameters TP, FN, TN and FP, in respect to the position of the buffer-zone around the reported landslide point. TP, FN, TN and FP change within the extension of the buffer zone.

465 Since the reference data on historical landslides come from several sources, the localization of the instability could not be geo-localized with high precision. Moreover, landslide localization is sometimes missed and only scarce information about the municipalities hit can be retrieved by archives (ISPRA, 2018; Inventario Fenomeni Franosi). Therefore, the reference data should be elaborated on and sometimes corrected. The historical landslides are generally represented on a map by a point in correspondence with the crown. To retrieve the effective landslide spatial extension (e.g. the destabilized area), an intersection

470 with the IFFI polygons was done. Unfortunately, not every point has corresponded to 1 landslide, and this may relate to the incompleteness of the IFFI catalogue and the approximation of the point positioning. In order to carry out the ROC methodology, avoiding these issues in reference data, a buffer zone with different radii around each landslide point was created: 250 m, 500 m, 1000 m and 2000 m (Figure 5). This radius represents an attempt for considering the uncertainties about the real position of the triggered landslide. As reported in Figure 5, each failure detected by CRHyME inside the buffer zone

475 should be assumed as a true positive (TP) for the ROC assessment. On the other hand, the false positive (FP) is represented by the cells inside the buffer zone that have not experienced any instability during the event. As a result, it was also possible to identify the true negative cells (TN), which represent the cells outside the buffer that were not destabilised and, on the opposite, the false negative (FN) cells.

2.4 Cases Studied

480 The case studies considered for calibration and validation of the CRHyME model are the Valtellina catchment of Adda river, and the Emilia area with Trebbia, Nure and Parma catchments. These areas raised our interest because in the past have experienced serious geo-hydrological problems caused by intense rainfall episodes:

- The Valtellina valley (Figure 6) is comprised of the northern part of the Lombardy region and in 1987 experienced a dramatic geo-hydrological episode triggered by rather intense and prolonged rainfalls. The Adda catchment

485 experienced a huge flood in correspondence with the middle part of the valley and a floodplain was entirely flooded by 3 m of mud and sediments. The effects on the territory were severe: shallow landslides, debris flows, and flash floods were recorded causing human injuries; 35 fatalities; and extensive damage to infrastructure and buildings, estimated at EUR 2 billion. A similar episode iteratively hit the area also in November 2000 and 2002 causing extensive damages across the entire province, especially on a little village situated on a foot hill, but with a lower

490 magnitude than in 1987.

- The Emilia area (Figure 6) has experienced similar geo-hydrological episodes like Valtellina respectively in October 2014 and September 2015. Three watersheds were particularly affected: Trebbia, Nure and Parma catchments. In both events, the territory experienced the triggering of several shallow landslide movements that have evolved in many cases to debris flow and flash floods causing problems also to Piacenza and Parma cities situated downstream. The

495 event of October 2014 hit the Parma catchment while the event of September 2015 hit the Trebbia and Nure catchments.
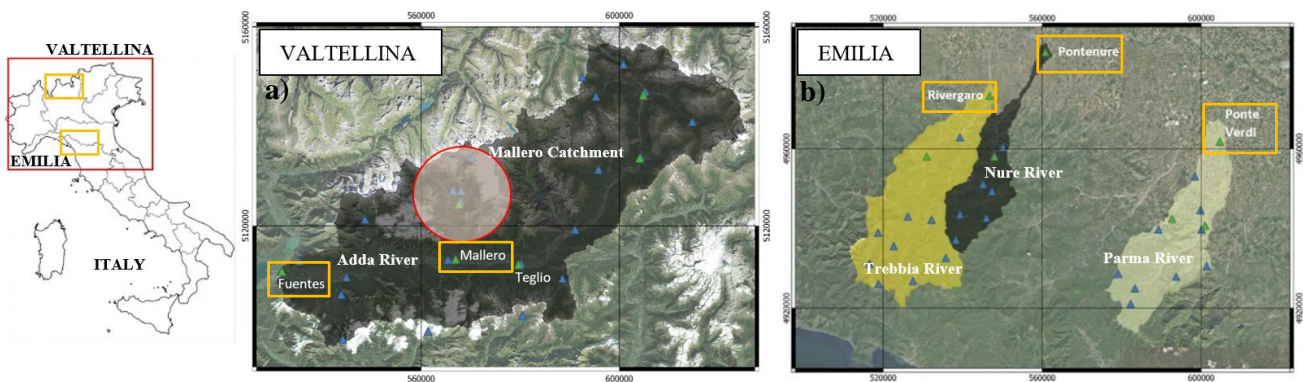
Figure 6: a) Valtellina and b) Emilia case study. In the red circle is highlighted the Mallero catchment and in orange boxes are the hydrometer stations considered for assessing the CRHyME performances: Fuentes and Mallero hydrometers for Valtellina and

500 Rivergaro (Trebbia), Pontenure (Nure) and Ponte Verdi (Parma) for Emilia. Base layer from © Google Maps 2023.

Monitoring points have been chosen in correspondence with the reference hydrometers situated at catchment outlets (Figure 6) that have been considered for checking the water discharge and volume. Hydropower reservoirs and literature studies were considered for evaluating solid transport. Regarding the shallow landslide and debris flow detection, a literature survey has been conducted to find a precise census of the occurred failure during the selected events. The census has been later compared

505   with the detected failures in CRHyME. For the water flow and solid transport comparisons at monitoring points, the NSE and RMSE index were considered while the ROC curves were adopted for evaluating the landslide and debris flow failures detection over the catchment area.

The simulations in the two cases were carried out following this scheme:

- Previously, a long-term simulation (LT) of 2-3 years has been assessed to rise the model to a realistic initial condition.
510   The former is necessary for water redistribution across the catchment that is necessary to achieve the river formation on the valley bottom, the moisturizing of superficial terrain and the recharge of groundwater. A redistribution of the erodible material according to the Gavrilovic model is also necessary for the correct reproduction of sediment transport.

- Then, a short-term simulation (ST) was conducted in correspondence with the main geo-hydrological event described
515   before. For the Valtellina, the events of July 1987, November 2000 and November 2002 have been reproduced considering a restarting condition coming from LT simulations. For the Emilia case study, the events of October 2014 and September 2015 were tested respectively in Parma and Nure, Trebbia catchments.

3 Results

In the following paragraphs the results of the CRHyME model simulations are reported

520   ## 3.1 Valtellina Case Study

The analysis conducted for the Valtellina area has followed the steps reported in Table 2.

	Starting Date	Ending Date	Rainfall Dataset used
Calibration	01/09/2015	31/08/2018	ARPA Lombardia and MERIDA
Validation	01/09/2018	31/12/2019	ARPA Lombardia and MERIDA
1987 event	01/09/1984	31/07/1987	ARPA Lombardia
2000 event	01/09/1997	30/11/2000	ARPA Lombardia
2002 event	01/12/2000	31/12/2002	ARPA Lombardia

Table 2: Simulation settings of Valtellina case study. The first calibration and validation of the model have considered more than 4 years of data on daily basis gathered from ARPA (Environmental Agency) (Rete Monitoraggio ARPA Lombardia) weather stations
525   **and the MERIDA reanalysis database (Bonanno et al., 2019). These event-based simulations were carried out for significant geo-hydrological events of July 1987, November 2000 and November 2002.**

The CRHyME calibration for Valtellina has been carried out for three years comprised between 1 September 2015 and 31 August 2018. Then, a subsequent validation period started on 1 September 2018 up to 31 December 2019. In Figure 7 the

water discharge and the total volumes computed by CRHyME in the two reference sections of Fuentes and Mallero are
530   reported. In addition, two different meteorological datasets were examined:

- The first one has considered the meteorological data provided by the Regional Agencies for Environmental Protection (ARPA Lombardia) (Rete Monitoraggio ARPA Lombardia) ground-based weather stations. Around 25 weather stations located in the Valtellina area have been selected for simulations considering a temporal resolution of 1 day and spatially interpolated with IDW (inverse distance weight) technique (Chow et al., 1988). The former has been

535   selected to make the simulations consistent with the past series available for 1987, 2000 and 2002 events, recorded on daily basis,

- The second one has taken into account MERIDA, the MEteorological Reanalysis Italian Dataset (Bonanno et al., 2019). MERIDA consists of a dynamical downscaling of the new European Centre for Medium-range Weather Forecasts (ECMWF) global reanalysis ERA5 using the Weather Research and Forecasting (WRF) model, which is

540   configured to describe the typical weather conditions of Italy. The optimal interpolation (OI) technique is applied to the modelled 2 m temperature and precipitation data using meteorological observations of the Regional Agencies for Environmental Protection (ARPA) in order to obtain ad 2D field of meteorological variables.
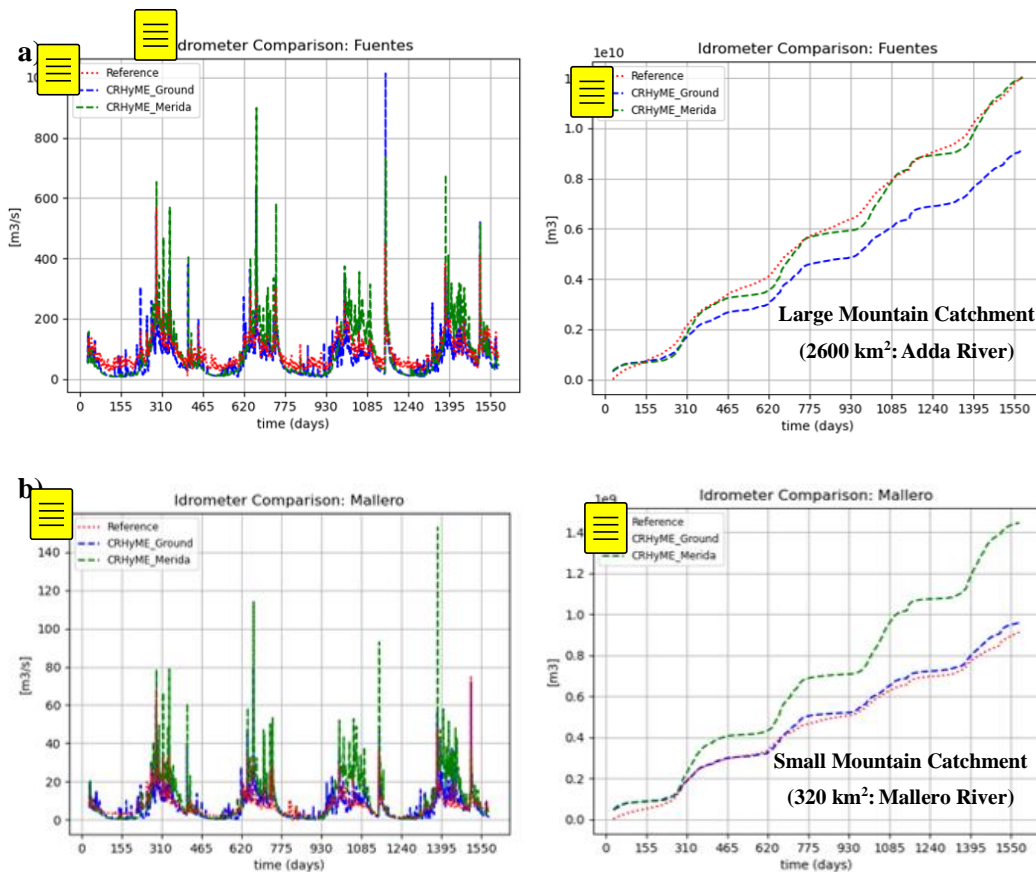
545

Simulation 2015-2019	NSE [-]	RMSE [mm]	NSE_MERIDA [-]	RMSE_MERIDA [mm]
Q Fuentes	0.199	45.370	-0.603	64.172
V Fuentes	0.783	$1.587 \ 10^9$	0.993	$2.931 \ 10^8$
Q Mallero	0.325	4.695	-2.369	10.494
V Mallero	0.988	$2.852 \ 10^7$	-0.145	$2.736 \ 10^8$

Figure 7: CRHyME model simulation results of water discharges (left) and liquid volume (right) at Fuentes (a), and Mallero hydrometers (b), for the period 2015-2019. Performance index running the model CRHyME using Ground-Based weather station and MERIDA dataset for the period 2015-2019. As can be appreciated, the Volume performances are better that Discharge performance: the Valtellina basin is strongly regulated by hydropower plants and dams that operate a consistent lamination of the peak discharge during major rainfall events; the kinematic routing may be not sufficiently accurate for flood propagation across the valley floodplain since dynamic lamination may occur. As a result, green and blue spikes overestimate the peak discharge with respect to the reference hydrometer.

Looking at the NSE, which is the most representative index for assessing data series agreements, for simulation carried out with the ARPA dataset, the total volume cumulated at Fuentes and Mallero sections (blue) is comparable with the reference line (red) calculated at the hydrometers. In all two cases, NSE is comprised between 0.9 and 1 a so it is very close to the perfect agreement. The model mass-balance conservation has been always checked in CRHyME to avoid and detect numerical model instabilities that may influence the water balance computation at the basin scale. In this light, the higher values of NSE represent a confirmation of the model conservativity. Regarding the water discharge, it can be noticed that the NSE has dropped dramatically from around 0 value. It seems that the model is not able to correctly reproduce the water discharge in terms of the peak of water flow. This is also confirmed by the large numbers of RMSE, especially for Fuentes's control point where the estimated error has the same order of magnitude as the Adda mean water discharge.

Looking at the scores with MERIDA dataset, we can observe a better agreement for the volume at Fuentes station while the performances are worse at the Mallero section. For the water discharges, the results have a lower agreement with respect to the reference and it can be glimpsed directly from the unphysical spikes (green) that were simulated by CRHyME. RMSE confirm the trend where errors are higher for the Mallero section rather than the Fuentes section. In this regard, the ARPA dataset has been taken into account for the geo-hydrological hazard quantification.

The calibration of the solid routing in CRHyME has followed these steps. Firstly, the catchment erosion has been evaluated using the Gavrilovic model predisposing all the erosion factors required by the method. A contingency table has been built in order to correlate the Z coefficient with the land use maps. Then, the model has been run to evaluate the sediment discharge through the TL (Transport Limited) and EL (Erosion Limited) methods and the results have been checked in correspondence with three hydropower reservoirs of Campo Tartano, Valgrosina and Cancano. For each reservoir, a literature survey has been conducted to estimate the sediment accumulation inside (Ballio et al., 2010; Milanesi et al., 2015).

The calibration parameter for sediment yield tuning is mainly represented by the D_{50} diameter that in our case has been expressed as a power-law continuous function of the slope (Figure 8). Since it doesn't exist a close formulation for indirectly

estimating the granulometry in absence of a field survey dataset different functions have been proposed taking into account literature surveys and approaches proposed by (Nino, 2002; Sambrook Smith and Ferguson, 1995; Lamb and Venditti, 2016; Berg, 1995). Several $Slope - D_{50}$ relations were retrieved from the studies and obtained varying the parameters of the curves. These relations mimic the functions proposed by (Berg, 1995) where the D_{50} is determined as a function of the river

580 morphology evolution, varying the two power-law coefficients. Among others, the set n°6 was sufficiently representative for the Valtellina area. In fact, the sediment yields yearly based have been matched with respect to the available data of Tartano (-11.7%), Valgrosina (+2.15%) and Cancano (-11.9%) dams.
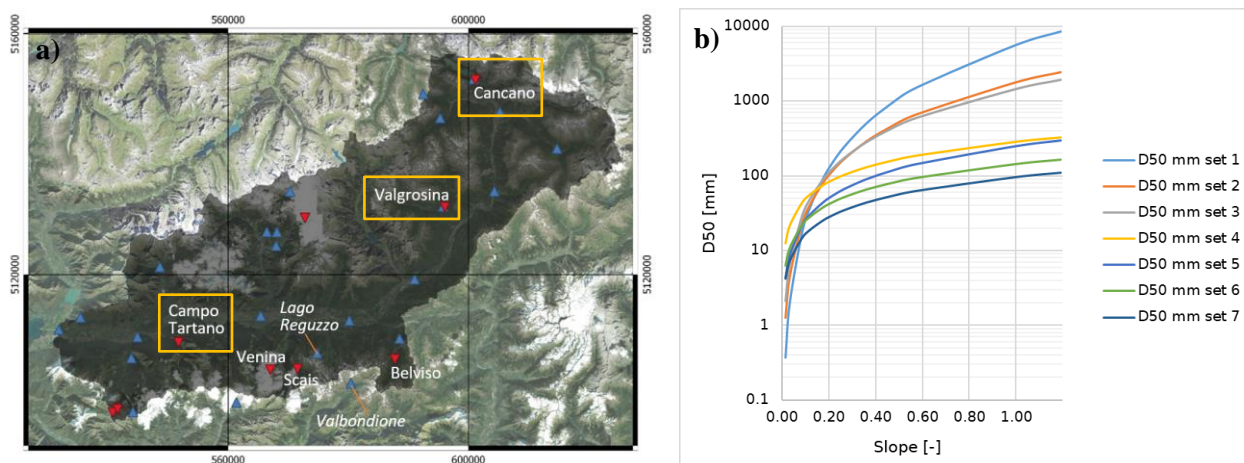
c)

Curve Set	a parameter	b parameter	Empirical Equations	Reference
Set 1	5604.8	2.38	$D_{50} = 5604.8\,Slope^{2.38}$	From (Berg, 1995), b = 2.38
Set 2	1786.9	1.79	$D_{50} = 1786.9\,Slope^{1.79}$	Decreasing a and b
Set 3	1453.1	1.61	$D_{50} = 1453.1\,Slope^{1.61}$	Decreasing a and b
Set 4	285.3	0.8	$D_{50} = 285.3\,Slope^{0.80}$	Decreasing a
Set 5	246.7	0.8	$D_{50} = 246.7\,Slope^{0.80}$	Decreasing a
Set 6	142.6	0.8	$D_{50} = 142.6\,Slope^{0.80}$	From (Nino, 2002), b = 0.8
Set 7	95.1	0.8	$D_{50} = 95.1\,Slope^{0.80}$	Decreasing a

d)

Sediment Yield	Campo Tartano Dam	Valgrosina Dam	Cancano Dam
Reference	38'037 m³/yr	33'600 m³/yr	21'450 m³/yr
Simulated 2015-2019	33'604 m³/yr	34'324 m³/yr	18'893 m³/yr
%	-11.7 %	+2.15 %	-11.9 %

585

Figure 8: **: a) Valtellina case study area where blue triangles represent rain gauge stations while red triangles are hydropower reservoirs; b) and c)** $Slope - D_{50}$ **relations tested and implemented in CRHyME based on the theory of** (Berg, 1995; Nino, 2002) **and considering on-site surveys; d) Sediment Yield estimations for three dams of Campo Tartano, Valgrosina and Cancano (orange boxes) where can be noticed the correct estimation with respect to the ITCOLD reference (ITCOLD, 2009, 2016). Base layer from**
590   **© Google Maps 2023.**

The correct localization of the shallow landslide triggered during the events of 1987, 2000 and 2002 events have been investigated by the ROC scores. The maps of Figure 9 describes the areas of application of ROC assessment for the shallow landslides that occurred in Valtellina during the July 1987, November 2000 and November 2002 events. At first sight, the
595   distribution of the shallow landslides interested all the provinces in all three events. Regarding July 1987 can be noticed a not uniform mapping of the failures was taken from the IFFI database. Shallow movements seem to be distributed only in the middle sector of the valley and decrease abruptly on the adjacent sides. For 2000 (orange) and 2002 (purple) events, the distribution has been reconstructed (Dapporto et al., 2005; Crosta and Frattini, 2003), integrating the information stored in the IFFI database. As can be appreciated in Figure 9, the distribution is much more uniform and has interested the slopes in the
600   bottom part of the relief, in correspondence with the vineyard cultivations.
As a first ROC assessment, a comparison among the four-landslide instability models has been carried out. To do that a realistic combination of friction angle values has been considered for the area: 40° for gravels, 35 ° for sand, 33° for silt and 30° for clay. To obtain a spatial distribution of the friction angle, this combination has been weighted by considering the fraction of soil composition, retrieved directly from available soil data. A minimal threshold of 30° that corresponds to a friction angle
605   for compacted organic terrain was considered not to lower excessively the stability of slopes in dry conditions. Then, each stability model (Iverson, Harp, Milledge and SLIP) has been tested for the three reference events of 1987, 2000 and 2002 and considering different buffer extensions of 250 m, 500 m, 1000 m and 2000 m. Among others, the Harp model has performed best with respect to the others, followed in the order by Milledge, Iverson and SLIP models. In Figure 9 are reported the results obtained by Harp model varying the buffer extension around the census landslide point.

610
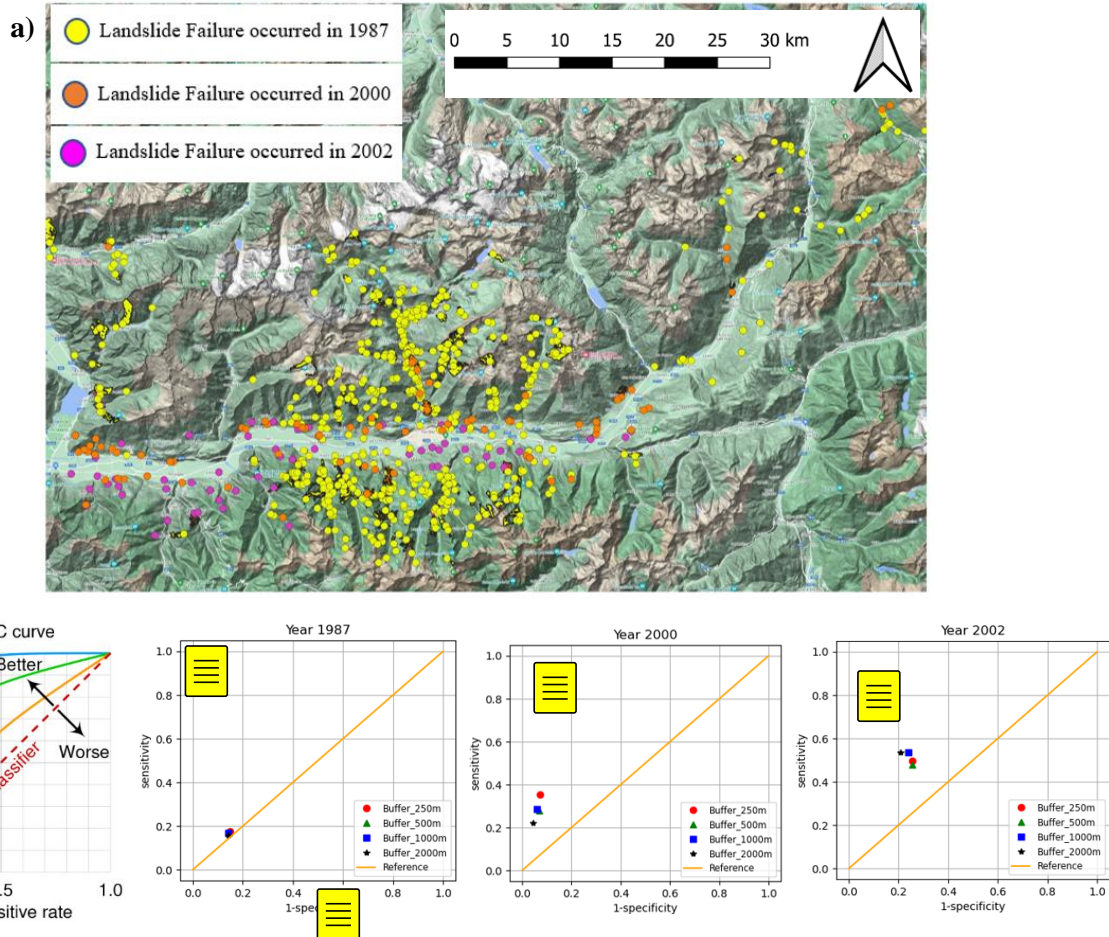
Figure 9: a) Triggered shallow landslides during the events of July 1987 (yellow points), November 2000 (orange points) and November 2002 (fuchsia points) across the Valtellina area from (Inventario Fenomeni Franosi). b) ROC curves for 1987, 2000 and 2002 events considering the model Harp. Base layer from © Google Maps 2023.

In every case, the ROC curves have assessed a model performance above the "random classifier" threshold line. The sensitivity (True Positive Rate) of the model is generally comprised of between 0.2 and 0.6 while the 1-specificity (False Positive Rate) is around 0.2. The distorted distribution of the shallow landslide census related to 1987 may have influenced the performance predictions, lowering the ROC assessment with respect to 2000 and 2002 events. The choice of the buffer extension can influence the redistribution among TP and FP and generally, the performance may tend to lower when large buffers are considered, especially for 1000 m and 2000 m radii. On the other hand, the radius of 250 m and 500 m are closest to the actual extension of shallow landslide movements. For the examined case studies, the model has shown a good ability to correctly individuate the location of the triggered landslide.

3.1 Emilia Case Study

625 For the Emilia case study, CRHyME was tested following a similar procedure schedule for Valtellina area. Simulations were carried out considering a period of 5 years from 01/09/2011 up to 31/12/2015 where geo-hydrological events of 13/10/2014 and 14/09/2015 have been recorded in the area (Table 3).

	Starting Date	Ending Date	Rainfall Dataset used
Trebbia	01/09/2011	31/12/2015	ARPA Emilia
Nure	01/09/2011	31/12/2015	ARPA Emilia
Parma	01/09/2011	31/12/2015	ARPA Emilia

Table 3: Simulation settings of Emilia case study considering the ARPA Emilia (Rete Monitoraggio ARPA Emilia)

630 After running CRHyME for the entire simulation period, keeping the calibration parameters assessed for the Valtellina case study, the model scores have been examined. The hydrology of Trebbia, Nure and Parma rivers has shown better scores in water discharge reproduction for the tested period. Looking at NSE, we can appreciate that higher scores are assessed for the water volume especially for Nure (0.978) and Trebbia (0.773) rivers while for Parma large errors were shown (0.482). However, with respect to Valtellina area, the scores for water discharges are sensibly better for Trebbia (0.272) and Parma

635 rivers (0.452) while for Nure the scores are lower, also confirmed by the RMSE index (Figure 10).

Looking at the solid transport quantification, the AdBPo (Autorità di Bacino del fiume Po) (Autorità di Bacino Distrettuale del Fiume Po, 2022) estimations obtained for the three basins have been taken into consideration for the comparisons. The AdBPo data were calculated by applying the EPM. Keeping the calibration of the D50-slope curve that was adopted for Valtellina, the results obtained after the simulations has shown good accordance with respect to the reference. In the three cases, the order of

640 magnitude of the sediment yield delivered each year at the outlet is similar to AdBPo data especially for Trebbia (+12.6%) and Parma (-24.7%) basins while for Nure we have a slightly larger difference (-35.7%).

645

650

		NSE	RMSE
Q Rivergaro		0.272	27.915
V Rivergaro		0.773	5.450 10^8
Q Pontenure		0.102	33.468
V Pontenure		0.978	3.765 10^7
Q Ponte Verdi		0.452	14.898
V Ponte Verdi		0.482	3.704 10^8

Sediment Yield	Trebbia
AdbPo Reference	247.2 10^3 m^3 yr^{-1}
Simulated	278.3 10^3 m^3 yr^{-1}
%	+12.6 %
Nure	Parma
69.4 10^3 m^3/yr	101.1 10^3 m^3 yr^{-1}
44.6 10^3 m^3/yr	76.1 10^3 m^3 yr^{-1}
-35.7 %	-24.7 %

655
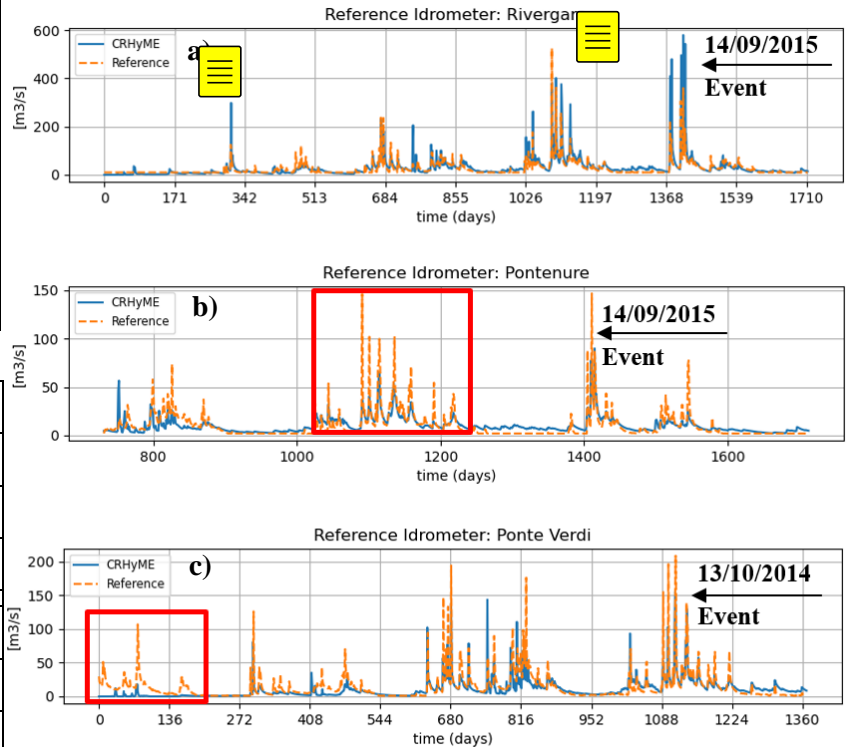
Figure 10: CRHyME model simulation results of water discharges, liquid volume, solid discharge, and solid volume at a) Rivergaro (Trebbia), b) Pontenure (Nure), c) Ponte Verdi (Parma) for the period 2011-2015. In the red box "A" are highlighted the peak discharge overestimation for Nure river. In the red box "B" are highlighted the weak performance of CRHyME for the Parma catchment at the beginning of the period due to initial condition uncertainties.

660 The ROC analysis has assessed the performance of CRHyME in detecting the triggered debris flow during the events of October 2014 and September 2015 (Figure 11). In this case, a short sensitivity analysis on the value of the friction angle was carried out since the value provided for Valtellina seems to be too conservative with respect to stability. Among the different simulations carried out, the best scores were obtained for a slightly decreased friction angle: 34° for coarse fragments, 28° for sand, 20° for silt and 30° for clay. This choice is in accordance with the hypothesis that debris flow can be triggered if 665 incoherent deposits are generally more prone to failures than terrain slopes. In most cases the model has outperformed the random classifier, showing a sensitivity (true positive rate) comprised between 0.1- 0.4 and a higher value of specificity depending on the chosen buffer extension around the triggering point. In our simulations, debris flow failure has been effectively highlighted across a small valley impluvium confirming the onsite observations carried out by (Ciccarese et al., 2020; G. et al., 2021).

670
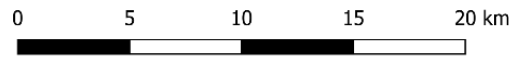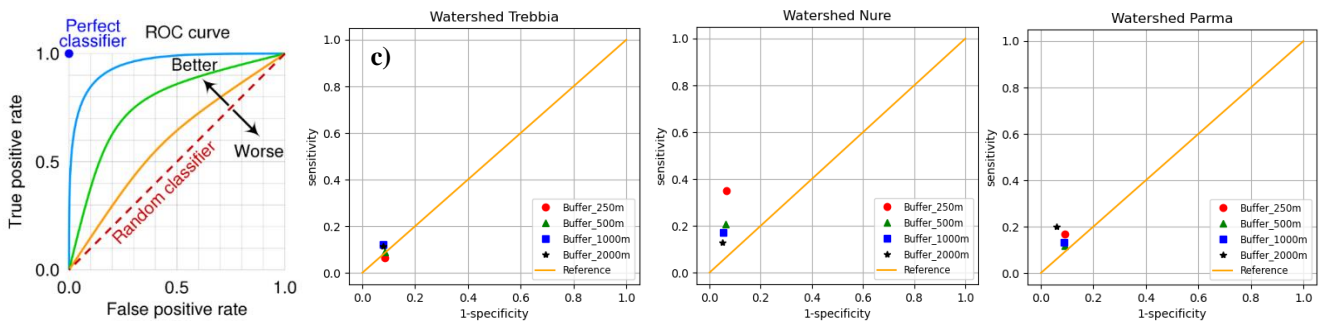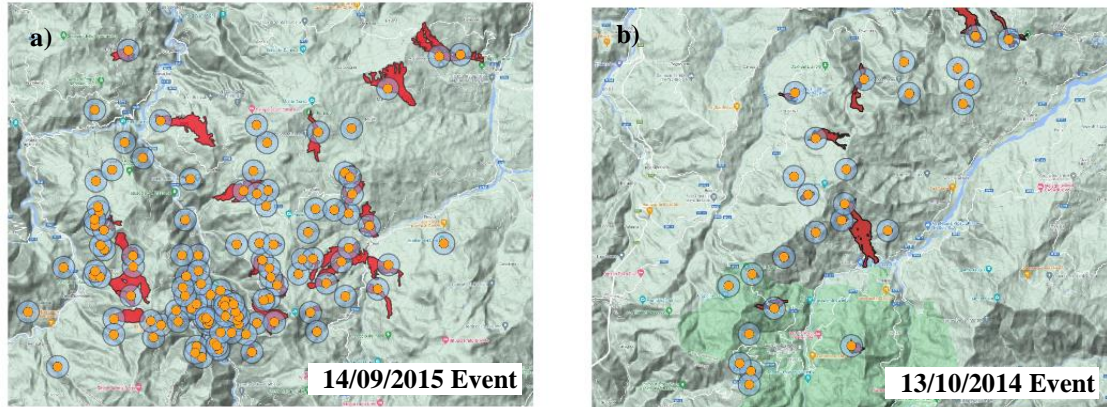
Figure 11: a) Trebbia-Nure landslide triggered during the event of September 2015 (left), b) Parma-Baganza landslide triggered during the event of October 2014 (right). Orange points are the triggering starting point, blue circles represent a buffer around the point and red polygons are the IFFI landslide census mapped in the area and c) ROC curves for Trebbia, Nure and Parma watershed for the debris flow events of October 2014 and September 2015. Base layer from © Google Maps 2023.

675

4   Discussion

4.1 The hydrological performance of Valtellina and Emilia case studies

As shown in the previous paragraph, CRHyME hydrological performances are not particularly satisfactory regarding the water

680 discharge reproduction (NSE ~ 0.2-0.3), especially for the case study of Valtellina considering both ARPA and MERIDA datasets. The characteristics of Valtellina catchments, where river discharges are regulated by the presence of a consistent group of hydropower plants (ITCOLD, 2009, 2016) can decrease the CRHyME performances in reconstructing the water discharges peaks recorded at the outlet. In fact, in the current version of the model lakes and dams are not considered since still data about how they operate and flood regulations are not available to the public. On the other hand, the kinematic routing

685 of runoff, which is sufficiently representative of the small lateral catchment rainfall-runoff processes (Chow et al., 1988), maybe not be suitable for interpreting floodplain flood evolution where dynamic routing should be considered. In fact, due to its morphology, Valtellina valley has a rather long floodplain (70 ~ 80 km) where larger river sections are present together

with 4 in-line reservoirs that can operate important flood lamination during intense rainfall events. This explains the best score of the Mallero sub-catchment (NSE = 0.325) with respect to the Fuentes section (NSE = 0.199) related to whole Adda catchment.

As a counter-example, the hydrology of Emilia rivers has similar scores of Mallero in water discharge reproduction for the tested period with the best agreement for Trebbia (NSE ~ 0.27) and Parma (NSE ~ 0.45). These basins are less regulated by hydropower reservoirs with respect to the whole Valtellina, and, since they are smaller (about 1/3), also the kinematic approach for runoff routing is much more representative of the catchment behaviour. Nevertheless, for the Nure river, the lower scores are caused by the appreciable differences between CRHyME discharge peaks that overestimate during rainfall periods the ones recorded by the hydrometer, even though the catchment behaviour seems to be represented correctly thanks to the volume conservation (NSE ~ 0.978). Looking at Figure 5, Pontenure hydrometer is located across the flood plain ~20 km downstream of the catchment with respect to the Rivergaro (~1 km) and Ponte Verdi (~10 km) stations. Similar to Valtellina, a flood lamination is likely to occur before reaching the stations so a dynamic approach should be tested instead of kinematic routing in order to increase the discharge agreements.

The higher performances in the volume quantification obtained by CRHyME in almost all tested cases (NSE ~ 0.8-0.9) assure that the routine is numerically and hydrologically conservative. Numerical stability has been guaranteed by built-in PCRaster libraries adopted for computations where some stability criteria have been matched especially for kinematic and dynamic routing functions. Since hydrological balance and water redistribution across the catchment domain are rather articulated, CRHyME calculates the ratio among the water Inflows and Outflows at each time step: if the model works numerically conservatively it is kept equal to 1. The high value of the NSE index has shown that the behaviour of the catchment dynamic over a long period of simulation is correctly interpreted. This is true especially for the Valtellina case study, using the ARPA dataset, and for Trebbia and Nure basins while only for Parma the score was sensible lower. A possible explanation may reside in some errors that affected the early simulation period where the CRHyME model has not already reached the regime condition giving a non-optimal reconstruction of the water discharge.

Comparing volume and discharge scores a general tendency to overestimation of the peak discharge during rainfall seasons can be noticed while an underestimation of the discharges during winter is detected. The main reason should be imputed also in part to the water recirculation inside the groundwater reservoir that, as already anticipated in section 2, has been included bearing in mind several assumptions due to the data scarcity and hydrogeological uncertainties. In this regard, Alps and Apennines have a different geological history that may affect the groundwater dynamics and this aspect may have not been glimpsed totally by the Dupuit model implemented in CRHyME. Unfortunately, the unavailability of reference piezometric data has not permitted us to assess model performance for this part.

4.1.1 Precipitation uncertainties: datasets across the Alps

Correctly assessing the precipitation distribution is mandatory to define a realistic representation of the external forcing that influences mainly the dynamic of the geo-hydrological cycle (Abbate et al., 2021b). Unfortunately, especially across mountain

regions, the higher local variability of meteorology and the absence of a distributed network of stations can complicate the reconstruction of a continuous field, especially for rainfall. Differences were appreciated using two different datasets for the Valtellina case study, revealing that ARPA stations are settled ground-based and represent the most accurate indication of the effective rainfall drop into the soil surface. The former is the data required by CRHyME and in this sense, reanalysis data such as ones from MERIDA (Bonanno et al., 2019) are preferable because they already produce precipitation as a spatially distributed map, covering also area without rain gauges. Using MERIDA, we would expect a better performance from CRHyME runs but this hypothesis has not been confirmed in all situations. Looking at water volumes transited across the Fuentes hydrometer during the period 2015-2019, the MERIDA dataset has performed better than ARPA stations with respect to the reference. On the other hand, looking at the Mallero hydrometer, the MERIDA dataset has scored worse rather than using directly ARPA stations. What is the possible explanation for this contradictory fact?

The main difference resides in the different reconstructions of the rainfall field from the two datasets since the model has driven the simulations by keeping the same calibration parameters. MERIDA gives an already corrected rainfall map that has a spatial resolution of 4 km while the ARPA stations data are interpolated geometrically using the Inverse Distance Weight (IDW) techniques. The former is a good interpolator when the network density is rather high and uniformly distributed across the landscape and this is a good and fast solution for flat areas while across complex terrain, the orography can increase the errors in IDW (Abbate et al., 2021b). In the Valtellina case study, since it is a valley without a uniform rain gauge network, the IDW method has performed worse than MERIDA. Nevertheless, the power of MERIDA is valid if the watershed is rather large, while the performance may decrease for a smaller basin. In the Valtellina case study, this situation has emerged for the Mallero catchment (Figure 5) that represents a branch of the main reach Adda. Analysing the water discharge volume, across the Mallero basin, MERIDA has performed worse rather than IDW. In this case, the coarse resolution of MERIDA has represented a critical point while the rainfall field has been reconstructed in a better way by local ARPA stations. It is important to mention that the Mallero catchment is a well-monitored basin where around ~10 weather stations are distributed across an area of 320 km^2 so that IDW can interpolate better the precipitation field. This evidence is following some literature studies (Abbate et al., 2021b; Bonanno et al., 2019; Ly et al., 2013) where the problems related to the smoothing of the rainfall peak operating by meteorological models are highlighted.

4.1.2 Initial hydrological condition uncertainties

The choice of a realistic initial condition for the catchment's soil moisture and its dependence on rainfall field reconstruction represents a common problem for a deterministic model (Uber et al., 2018; Tramblay et al., 2010; Chow et al., 1988). In some cases, it is very difficult to have sufficient measures about the superficial water content of the soil, groundwater piezometric and superficial discharges. Regarding water flows, precise quantification of the discharge is generally produced by hydrometers that are normally located at the outlets of the basins. These data series are barely distributed and sometimes may fail to give useful data, especially during extreme events where they may be discontinued due to a lack of electric power.

Finally, soil moisture is a quantity that can vary abruptly across different terrain types, so it is not common to implement a
network that permits the acquisition of distributed information across a catchment (Lazzari et al., 2018).

755 In CRHyME, these problems have been in part skipped considering that the model reached an automatic adjustment after some
time steps that, depending on the extension of the basin, can be comprised of a few months up to some years. The former is a
sort of automatic autocalibration of the model. In fact, the long-run simulation permits a distribution of the water across the
cells of the domain (horizontally) and across each layer of the model (vertically). This effect was rather evident for the Emilia
case study, where a realistic regime condition was reached only after a couple of years, and it was rather slower than for the

760 Adda basin. The regime conditions have been acquired less rapidly since to the different soil compositions and morphology
between the two areas. In the Apennines, the presence of clay can generally decrease the speed of soil saturation slowing down
the groundwater recharge (Ronchetti et al., 2009; Ciccarese et al., 2020). As a result, the regime condition can take several
times with respect to the Alps, where coarser terrain granulometry can reduce it due to higher soil permeabilities. Two-three
years are generally sufficient to reach a regime condition since the fact that liquid discharge recorder at the outlets starts to

765 match the hydrometric series.

4.2 The geo-hydrological performance of Valtellina and Emilia case studies

4.2.1 Solid Transport

Regarding the geo-hydrological hazard quantification, bearing in mind the limited availability of historical and reference data
and their embedded uncertainties, landslide and solid transport processes have been reproduced with good affordability. The

770 sediment yields calculated on a yearly based have been matched with respect to the available data of Tartano, Valgrosina and
Cancano dams after a calibration procedure that has involved the application of the function for redistributing D_{50} grain size
parameter across the catchment. The good reproduction of the annual sediment yield (~ 10% underestimation for Valtellina)
has been confirmed also for the Emilia case study where the order of magnitude was correctly reproduced with respect to
AdBPo reference (± 20% depending on the basin).

775 Since the D_{50} is embedded into the threshold that activates the sediment transport (Vetsch et al., 2018), it has revealed the
critical parameter to be assessed in the CRHyME model. In the literature, there is plenty of studies that have investigated the
dynamic of solid transport, but they lack giving a comprehensive theory that could be applied in those case where field data
are not available. The empirical formulation proposed for CRHyME is an attempt in this direction, but since it is a currently
open problem further research is planned for future versions of the model.

780

4.2.2 Shallow landslide and debris flow

The CRHyME model has identified correctly the localization and the timing of landslide failure during the extreme events that
have affected the studied catchment. For the Valtellina area, 1987, 2000 and 2002 events were reproduced consistently by
looking at ROC scores. The best scores were acquired for 2000 and 2002 events also a good quality census was available for

785 the investigated area. For 1987, as can be appreciated in Figure 9, the incompleteness of the available census (yellow points)

has affected the model's final score. However, independently from the specific case, the ROC methodology has permitted us to highlight how the choice of stability parameters (friction angle and cohesion) has a critical influence on the final results. This fact has been confirmed also by the sensitivity analysis carried out for debris flow episodes in the Emilia case study during the event of 2014 and 2015. Here, in order to reach the best ROC scores with respect to the random classifier, the friction

790   angles calibrated for Valtellina have been slightly reduced by about 20%.

CRHyME experience has shown how landslides and debris flow stability assessment cannot be treated deterministically even with an infinite slope model equation if some key data are not available or tuned indirectly from the others. In particular, the friction angle of the natural slope, and the cohesion of the superficial soil represent the most uncertain parameters that unfortunately cannot be estimated even if a terrain sample is analysed in the laboratory. The former cannot be properly done

795   if the aim of the study is to investigate the slope stability at the catchment scale. Up to now, there are still few examples of the spatial distribution prediction of these two quantities that are essential for simulating geo-hydrological hazards, especially for landslide susceptibility mapping. In this regard, stochastic techniques are sometimes implemented to fulfil these needs (Vardon et al., 2016). In the simulations of Valtellina and Emilia case studies, a brief sensitivity analysis was carried out considering ranges given by the literature survey but without implementing a Montecarlo simulation of stability coefficients. The tuning

800   procedure is difficult since depends also on the large uncertainties that can be found inside the reference database that is used for validating the carried-out simulation. Moreover, friction angle depends on soil consolidation which is barely unknown while soil granulometry is the final result of the complex sediment dynamics and geological processes that have not been clarified at all (de Vente and Poesen, 2005; Merritt et al., 2003; Shobe et al., 2017; Ballio et al., 2010; Kondolf, 1997). Similarly, to the D_{50} parameter, these problems represent a research frontier that will be further strengthened in the future

805   version of the model.

4.3 Geo-hydrological uncertainties: superficial geo-hydrological cycle

CRHyME is intended to simulate superficial geo-hydrological processes occurring at the catchment scale. Through a multi-hazard approach is possible to quantify these phenomena giving insight into their potential effects on the territory, useful for engineering and Civil Protection purpose. In this regard, CRHyME is one of the first examples of an integrated model.

810   The existing methodologies used in the engineering field have the main drawbacks of threatening separately geo-hydrological processes, not giving a comprehensive framework of the geo-hydrological cycle (ISPRA, 2018; Vetsch et al., 2018; Ali et al., 2019; Gariano and Guzzetti, 2016). In literature, models that assess jointly the erosion processes with shallow landslide instabilities at the catchment scale are rare (Baartman et al., 2012; Roo et al., 1996; Van Der Knijff et al., 2010) since the approaches adopted, the data required for simulations and their availability have historically limited the applicability inside a

815   spatially-distributed model (Sutanudjaja et al., 2018; Strauch et al., 2018). Moreover, these processes have been studied in the past not always taking into account the high dynamicity of hydrological assessment, making strong assumptions on its stationarity, i.e. complete saturation of the slopes (Montgomery and Dietrich, 1994; Mandal and Maiti, 2015; Zhu and Xiao,

2020). In CRHyME, the hydrological aspect represents the main engine that, coherently with the observed reality, can trigger geo-hydrological instability at different locations and times.

820   Thanks to the PCRaster functions, CRHyME is a tool that overcomes the limitation related to lumped parameter erosion model, stream-power solid transport methodologies and to static susceptibility mapping for shallow landslide and debris flow. PCRaster permits to work with spatially distributed data and combine them to better describe the characteristic of a territory especially related to the local morphology, soil composition and coverages. Embedded routing functions are able to route the material (water or solid) through the whole catchment, extending the investigation of geo-hydrological in a spatial and time

825   perspective. Processes are not evaluated at a specific river section or single slope under the hypothesis of stationarity, but they are simulating through the entire domain and considering their transient. Moreover, CRHyME could produce dynamic susceptibility maps, highlighting for shallow landslide phenomena the area that could destabilise at a particular time-step of simulation, extending the concept of static susceptibility mapping where time components driven by meteorological triggering factors (rainfalls) are not always taken into account (Meisina et al., 2013; Ali et al., 2019; Atkinson and Massari, 1998; Benni

830   Thiebes et al., 2017).

According to (Gariano and Guzzetti, 2016), reconstructing the whole geological cycle that drives the superficial erosion process and landslide formation is a challenge. CRHyME model is not an exception: EPM semi-quantitative model is considered for simulating the erosion process while landslide and debris flow triggering do not involve their runout. The runout processes can redistribute the local terrain changing the soil depth (asportation at the crown and accumulation at the toe) and

835   modifying the DEM height. This dynamic is rather difficult to simulate consistently on a 2D domain even though a specific problem is addressed (Scheidl and Rickenmann, 2011). It represents one of the main assumptions for guaranteeing a fast functioning of the implemented routines in CRHyME: geo-hydrological assessment is computed after the hydrological assessment (one-directional sequence) and possible feedbacks, such as DEM modifications, are not taken into account up to now.

840   Uncertainties about hydrological simulations are present in CRHyME but can be "controlled" through the hydrometer stations if available locally. On the other hand, the assessment of the "superficial geological cycle" cannot be evaluated precisely since the monitoring of these geo-hydrological phenomena is still insufficient on a catchment scale (Inventario Fenomeni Franosi; ISPRA, 2018). Even though surface mapping and census are supposed to increase their accuracy and completeness in the future, some doubts remain about possible improvements in other fundamental data. To correctly assess the landslide

845   triggering, a uniform soil layer cannot be sufficient sometimes but further information about local geology in terms of lithological material, strata inclination and immersion and the eventual presence of faults should be included to have a complete picture of dynamics and triggering of the local geo-hydrological processes (Montgomery and Dietrich, 1994; Bovolo and Bathurst, 2012; Cevasco et al., 2014; D'Amato Avanzi et al., 2004). Up to now, these data are still represented in the geological sections that depict an accurate profile of the possible configuration of the layers. Unfortunately, geological sections are not

850   available digitally and cannot be included directly inside the models even though a complex 3D mesh is available and required by the program. The former is beyond the scope of CRHyME that can be in principle classified as a 2.5D model. Nevertheless,

the possibility to include those data could help in interpreting superficial and groundwater fluxes to reduce uncertainties, especially for larger catchments. In this sense, the databases already adopted in CRHyME (Hengl et al., 2017; Huscroft et al., 2018; Ross et al., 2018) have made an important homogenization of superficial soils properties that permit to implement in CRHyME stability models.

In conclusion, the deterministic reproduction of the "superficial geological cycle" poses some open problems still unresolved. Geo-hydrological processes cannot be perfectly coupled with the hydrological cycle since feedbacks are difficult to be taken into account and empirical formulations are necessary to try to simplify these complex interactions. CRHyME is one of the first attempts that aim to describe geo-hydrological processes coupled with hydrological dynamics deterministically and in an efficient way using the potentiality of PCRaster functions.

5 Conclusion

In this work, the new model CRHyME and its applications are reported. CRHyME model was built ex-novo with Python programming language taking inspiration from another open-source model PCR-GLOWB-2, also written in Python. Both models have the same framework and implement faster PCRaster libraries that can simulate hydrological processes in a very efficient way. CRHyME is characterized by 6 modules that reproduce water balance over terrain and an additional module deputed to simulate all the processes related to the geo-hydrological hazards (e.g. erosion, solid transport, shallow landslide and debris flow). CRHyME includes some of the common features of the classical hydrological model but with an additional focus on geo-hydrological hazards. Particular attention has been devoted to the study and to the implementation of the erosion and solid transport processes that can typically occur in a river catchment. Moreover, shallow landslide and debris flow stability models have been included. The integration of all those processes in a hydrological model represents a novelty in the field of geo-hydrological risk assessment. Of course, some hypotheses were assumed since it is quite impossible to implement accurately all the existent geo-hydrological mechanisms: some dynamics are still unknown or are too complex to be reduced to a 2D interpretation.

A model is affordable if correctly calibrated and validated. Calibration procedures are a critical part of the most common hydrological model since they measure how the results may be affected by the chosen parameters. Since the aim of our study was to build and use a model indistinctly in any area of the globe, the user-defined calibration parameters have been reduced to the minimum. In this way, we have reduced the possibility of parameter overfitting to a particular case study, making the CRHyME model rather general and usable in all catchments. Our case studies of Valtellina and Emilia were chosen with respect to the availability of historical data that is of paramount importance for validation: hydrometer discharges, bathymetric surveys from hydropower reservoirs and landslides census available in those areas have been considered in the simulations as reference data. The results have shown a good reproduction of the past observations: the model is hydrologically conservative (the volume of water recirculating across the basin is conserved), and numerically stable (thanks to PCRaster libraries); the solid discharge reproduced with downscaled EPM method is consistent with the observations, even though there are some

885 uncertainties on D_{50} parameter; the triggering of landslides is comparable in number and spatial localization with respect to the census data.

The efforts conducted in this study with the creation of CRHyME are in the direction of a better investigation and reproduction of geo-hydrological hazards. CRHyME is a multi-hazard model able to address and quantify at catchment scale several geo-hydrological processes that: may occur simultaneously, are physically coupled and cannot be interpreted separately. With CRHyME is possible to overcome the software fragmentation that is currently present in the geo-hydrological field, answering

890 the recent needs required for multi-hazard quantification and multi-risk evaluation not only for back analysis studies but also for now-casting evaluation at the Civil Protection level.

Appendix A

Here is reported an example of the CRHyME .INI file that was written for the computations. Each module has its options

895 where the parameters, variables and other settings required for the model run are specified.

```
[globalOptions]
inputDir = ***\ModelCRHyME\CRHyME_Inputs_Trebbia
outputDir = ***\ModelCRHyME\CRHyME_Outputs_R
cloneMap = map\clone.map
landmask = None
institution = RSE_Ricerca Sistema Energetico
title = CRHyME project
description = by Andrea Abbate and Leonardo Mancusi, resolution = 90 m
resolution = 90
startSeries = 1985-12-31
startTime = 1986-01-01
endTime = 2005-12-30
timestep = 24
startingStamp = 0
stampTimestep = 1
Restart = 1
Restart_Snow = \restarts\mod2\Restart_Snow.map
Restart_Surface = \restarts\mod2\Restart_Surface.map
Restart_Soil = \restarts\mod2\Restart_Soil.map
Restart_Ground = \restarts\mod2\Restart_Ground.map
Restart_SoilSed = \restarts\mod2\Restart_SoilSed.map

[climaOptions]
```

```
920  CLIMA_Switch = 1

     Rain_NC4 = netcdf\eucordhi_mod2_pr_day.nc

     CorrectionFactor = 86400

     [meteoOptions]
925  input_tab = tab

     mask = map\mask01.map

     DEM = map\dem_clip.map

     z0 = tss\mod2\Z0_eucordhi_mod2_tas_day.tss

     TempRatio = tss\mod2\TCoef_eucordhi_mod2_tas_day.tss
930  z0MAX = tss\mod2\Z0_eucordhi_mod2_tasmax_day.tss

     TempRatioMAX = tss\mod2\TCoef_eucordhi_mod2_tasmax_day.tss

     z0MIN = tss\mod2\Z0_eucordhi_mod2_tasmin_day.tss

     TempRatioMIN = tss\mod2\TCoef_eucordhi_mod2_tasmin_day.tss

     infilRain_file = tss\2011_2016\Rain_TREBBIA_Precipitazione_ALL.tss
935  mayrainstat = map\Rain_Stations_Trebbia.map

     LAT = 43

     ETC_Switch = 1

     Aspect = map\Aspect_Filled.map

     Slope = map\Slope_Filled.map
940  mysoilmap = map\CLC_9Cat.map

     Kc_FAO = tbl\Kc_FAO.tbl

     Albedo = tbl\Albedo.tbl

     [interceptionSnowOptions]
945  input_tab = tab

     LAImax = tbl\LAImax.tbl

     LAImin = tbl\LAImin.tbl

     SNOW_Switch = 1

950  [landSurfaceOptions]

     input_tab = tab

     INF_Switch = 2

     sand_sup = map\Sand_SUP90C.map

     silt_sup = map\Silt_SUP90C.map
955  clay_sup = map\Clay_SUP90C.map

     CoarseFrc_SUP = map\CoarsFrg_SUP90C.map
```

```
      myrivermap = map\PathRiverSM.map

      Loss_River = tbl\Loss_RIV.tbl

      Inf_CLC = tbl\Infiltr_CLC.tbl

960   CN_I = map\CN_I.map

      CN_II = map\CN_II.map

      CN_III = map\CN_III.map

      Initial_SM = 0.9

      SoilDepth = map\BDRICM_M.map

965   MaxWatStgTOP = map\TSH1_clip.map

      MaxWatStgBTM = map\TSH5_clip.map

      sand_btm = map\Sand_BTM90C.map

      silt_btm = map\Silt_BTM90C.map

      clay_btm = map\Clay_BTM90C.map

970   CoarseFrc_BTM = map\CoarsFrg_BTM90C.map

      [groundwaterOptions]

      input_tab = tab

      Sr_Falda = 0.8

975   Idro_Map = map\Idrogeology_Emilia_Trebbia.map

      Ks_GLHYMPS_exp = map\GLHYMPS_Emilia_Trebbia.map

      Permeability = tbl\IdrogeologyTabs\Permeability.tbl

      Anisotrophy = tbl\IdrogeologyTabs\Anisotrophy.tbl

      Porosity = tbl\IdrogeologyTabs\Porosity.tbl

980   Storativity = tbl\IdrogeologyTabs\Storativity.tbl

      Type_Depth = tbl\IdrogeologyTabs\Type.tbl

      [LandSlidesOptions]

      LANDSLIDE_Switch_1 = 2

985   C_Veg = tbl\C_Veg.tbl

      Surcharge = tbl\Sur_Veg.tbl

      fa_factor = 2

      X_Gavrilovic = tbl\X_Gavrilovic.tbl

      Y_Gavrilovic = tbl\Y_Gavrilovic.tbl

990   LithoY_Gavrilovic = map\Idrogeology_Emilia_Trebbia.map

      FI_Gavrilovic = map\Kst_Emilia_Trebbia.map

      [routingOptions]
```

```
         ROUTING_Switch = 1
995      lddMap = map\ldd_clip.map
         cellAreaMap = map\cellsizeArea.map
         River_Pit = map\Pit_Point.map
         Strickler = tbl\Ks_Strickler.tbl
         SectionTable = tbl\Dynamic\Sections2.tbl
1000     RiverDynPath = tbl\Dynamic\map\PathDyn.map
         RiverDynDist = tbl\Dynamic\map\DistDyn.map
         RiverDynPit = tbl\Dynamic\map\Pit_Point.map
         RiverDynPitLake = tbl\Dynamic\map\Pit_Point_Lakes_IN.map

1005     [reportingOptions]
         mysamples_real = map\Idro_Samples_Trebbia.map
         mysamples_fake = map\Idro_Samples_F.map
         mysamples_solid = map\Solid_Samples.map
         debugmode = FAST
1010     outDailyTotNC = CumFails,CumFails_D,P
         outMonthTotNC = P,ETc
         outMonthAvgNC = T
         outMonthEndNC = CumFails,CumFails_D
         outAnnualTotNC = P,ETc
1015     outAnnualAvgNC = T
         outAnnuaEndNC = CumFails,CumFails_D
         #debugmode = SLOW
         #outDailyTotNC = P,T,ETc,DeltaWS0,Sr3,DeltaBF0,FS,CumFails,FS_D,CumFails_D,FS_ST,CumFails_ST
         formatNetCDF = NETCDF4
1020     zlib = True
```

Appendix B

Here are reported all the symbols and their units of measure included in CRHyME model.

Main symbols	Description	Units of measurement
A	Hydraulic section area	m^2
B	Width of the hydraulic section	m
c	Cohesion of surface soils	kPa
C*	Concentration of debris flows	-

C_i	Canopy Interception	mm day^{-1}
CNI CNII CNIII	Curve Numbers SCS-CN for dry-mild-wet conditions	-
D_{50}	Median diameter of soil grain size	mm
ddf_0	Degree day factor	mm °C^{-1} day^{-1}
E_s	Surface erosion	mm day^{-1}o m^3 day^{-1}
Et_0	Potential evapotranspiration	mm
Et_c	Evapotranspiration	mm day^{-1}
E_x	Exfiltration	mm day^{-1}
f_0	Maximum infiltration rate of Horton	mm h^{-1}
f_c	Horton's minimum infiltration rate	mm h^{-1}
F_{gw}	Groundwater flow	m^{3}s^{-1}
F_{sub}	Subsurface flow	m^3 s^{-1}
h_{gw}	Groundwater height	mm
h_s	Surface ground height	mm
h_{snow}	Snow depth	mm
h_w	Water height at the surface	mm
h_{ws}	Water height in surface soil	mm
i o S	Dimensionless slope and degrees	% o °
I_a	Initial imbibition of the SCS-CN method	mm
k	Horton decay constant	h^{-1}
K_c	Crop Coefficient	-
K_s	Hydraulic permeability	m s^{-1}
K_{str}	Strickler roughness coefficient	-
LAI	Leaf Area Index	-
L_{per}	Percolation	mm day^{-1}
n	Porosity / Van Genucten n parameter / Manning coefficient	-
P	Rainfall	mm day^{-1}
P_n	Net Rainfall	mm day^{-1}
Q o ql	Liquid Discharge	m^3 s^{-1}
qc	Critical flow rate of incipient motion for solids	m^3 s^{-1}
qs	Solid flow rate	m^3 s^{-1}
R	Runoff	m^3 s^{-1}

S	Snow	mm
S	SCS-CN Storativity	mm
S_m	Snowmelt	mm day^{-1}
S_r	Soil Moisture	mm o %
T	Temperature	°C
T_{max} e T_{min}	Maximum and minimum temperature	°C
T_s	Solid Transport	m^3 s^{-1}
α e β liquido	Parameters of the uniform (liquid) flow rate curve	-
α e β solido	Parameters of the uniform (solid) flow rate curve	-
φ	Friction angle of surface soils	°
θ_s e θ_r	Maximum and minimum surface soil water content	mm o %

1025

References

Abbate, A., Longoni, L., Ivanov, V. I., and Papini, M.: Wildfire impacts on slope stability triggering in mountain areas, MDPI Geosciences, 9, 1–15, https://doi.org/10.3390/geosciences9100417, 2019.

Abbate, A., Papini, M., and Longoni, L.: Analysis of meteorological parameters triggering rainfall-induced landslide: a review of 70 years in Valtellina, Nat. Hazards Earth Syst. Sci., 21, 2041–2058, https://doi.org/10.5194/nhess-21-2041-2021, 2021a.

Abbate, A., Longoni, L., and Papini, M.: Extreme Rainfall over Complex Terrain: An Application of the Linear Model of Orographic Precipitation to a Case Study in the Italian Pre-Alps, 2021, MDPI Geosciences, 18, 2021b.

Abeshu, G. W., Li, H.-Y., Zhu, Z., Tan, Z., and Leung, L. R.: Median bed-material sediment particle size across rivers in the contiguous U.S., Earth Syst. Sci. Data Discuss., 2021, 1–22, https://doi.org/10.5194/essd-2021-201, 2021.

Ali, S., Biermanns, P., Haider, R., and Reicherter, K.: Landslide susceptibility mapping by using a geographic information system (GIS) along the China–Pakistan Economic Corridor (Karakoram Highway), Pakistan, Nat. Hazards Earth Syst. Sci., 19, 999–1022, https://doi.org/10.5194/nhess-19-999-2019, 2019.

Allan, R., Pereira, L., and Smith, M.: Crop evapotranspiration-Guidelines for computing crop water requirements-FAO Irrigation and drainage paper 56, 1998.

Alvioli, M., Melillo, M., Guzzetti, F., Rossi, M., Palazzi, E., von Hardenberg, J., Brunetti, M. T., and Peruccacci, S.: Implications of climate change on landslide hazard in Central Italy, Science of The Total Environment, 630, 1528–1543, https://doi.org/10.1016/j.scitotenv.2018.02.315, 2018.

1045 Ancey, C.: Bedload transport: a walk between randomness and determinism. Part 1. The state of the art, null, 58, 1–17, https://doi.org/10.1080/00221686.2019.1702594, 2020.

Anderson, E. I.: Modeling groundwater–surface water interactions using the Dupuit approximation, Advances in Water Resources, 28, 315–327, https://doi.org/10.1016/j.advwatres.2004.11.007, 2005.

Angeli, M. G., Buma, J., Gasparetto, P., and Pasuto, A.: A combined hill slope hydrology/stability model for low-
1050 gradient slopes in the Italian Dolomites, Engineering Geology, 49, 1–13, https://doi.org/10.1016/S0013-7952(97)00033-1, 1998.

Rete Monitoraggio ARPA Emilia: https://www.arpae.it/it/temi-ambientali/meteo.

Rete Monitoraggio ARPA Lombardia: www.arpalombardia.it/stiti/arpalombardia/meteo.

Atkinson, P. M. and Massari, R.: GENERALISED LINEAR MODELLING OF SUSCEPTIBILITY TO
1055 LANDSLIDING IN THE CENTRAL APENNINES, ITALY, Computers & Geosciences, 24, 373–385, https://doi.org/10.1016/S0098-3004(97)00117-9, 1998.

Autorità di Bacino Distrettuale del Fiume Po: Linee Generali di Assetto Idrogeologico e Quadro degli Interventi, 2022.

Baartman, J., Jetten, V. G., Ritsema, C., and de Vente, J.: Exploring effects of rainfall intensity and duration on
1060 soil erosion at the catchment scale using openLISEM: Prado catchment, SE Spain, Hydrological Processes, 26, 1034–1049, https://doi.org/10.1002/hyp.8196, 2012.

Ballio, F., Brambilla, D., Giorgetti, E., Longoni, L., Papini, M., and Radice, A.: Evaluation of sediment yield from valley slopes: A case study, 149 pp., https://doi.org/10.2495/DEB100131, 2010.

Bancheri, M., Rigon, R., and Manfreda, S.: The GEOframe-NewAge Modelling System Applied in a Data Scarce
1065 Environment, Water, 12, https://doi.org/10.3390/w12010086, 2020.

Bemporad, G. A., Alterach, J., Amighetti, F. F., Peviani, M., and Saccardo, I.: A distributed approach for sediment yield evaluation in Alpine regions, Journal of Hydrology, 197, 370–392, https://doi.org/10.1016/0022-1694(95)02978-8, 1997.

Benni Thiebes, Shibiao Bai, Yanan Xi, Thomas Glade, and Rainer Bell: Combining landslide susceptibility maps
1070 and rainfall thresholds using a matrix approach, RG, 19, https://doi.org/10.21094/rg.2017.003, 2017.

Berg, J. H.: Prediction of Alluvial Channel Pattern of Perennial Rivers, Geomorphology, 12, 259–279, https://doi.org/10.1016/0169-555X(95)00014-V, 1995.

Bonanno, R., Lacavalla, M., and Sperati, S.: A new high-resolution Meteorological Reanalysis Italian Dataset: MERIDA, Quarterly Journal of the Royal Meteorological Society, 145, 1756–1779,
1075 https://doi.org/10.1002/qj.3530, 2019.

Bordoni, M., Meisina, C., Valentino, R., Lu, N., Bittelli, M., and Chersich, S.: Hydrological factors affecting rainfall-induced shallow landslides: From the field monitoring to a simplified slope stability analysis, Engineering Geology, 193, https://doi.org/10.1016/j.enggeo.2015.04.006, 2015.

Bovolo, C. I. and Bathurst, J. C.: Modelling catchment-scale shallow landslide occurrence and sediment yield as a
1080 function of rainfall return period, Hydrological Processes, 26, 579–596, https://doi.org/10.1002/hyp.8158, 2012.

Bozzolan, E., Holcombe, E., Pianosi, F., and Wagener, T.: Including informal housing in slope stability analysis – an application to a data-scarce location in the humid tropics, Natural Hazards and Earth System Sciences, 20, 3161–3177, https://doi.org/10.5194/nhess-20-3161-2020, 2020.

Brambilla, D., Papini, M., Ivanov, V. I., Bonaventura, L., Abbate, A., and Longoni, L.: Sediment Yield in Mountain
1085 Basins, Analysis, and Management: The SMART-SED Project, in: Applied Geology: Approaches to Future Resource Management, edited by: De Maio, M. and Tiwari, A. K., Springer International Publishing, Cham, 43–59, https://doi.org/10.1007/978-3-030-43953-8_3, 2020.

Bresciani, E., Davy, P., and de Dreuzy, J.-R.: Is the Dupuit assumption suitable for predicting the groundwater seepage area in hillslopes?, Water Resources Research, 50, 2394–2406, https://doi.org/10.1002/2013WR014284,
1090 2014.

Buma, J.: Finding the most suitable slope stability model for the assessment of the impact of climate change on landslide in southest france, Earth surface processes and landforms, 25, 565–582, https://doi.org/10.1002/1096-9837(200006)25:6<565::AID-ESP101>3.0.CO;2-D, 2000.

Campforts, B., Shobe, C., Steer, P., Vanmaercke, M., LAGUE, D., and Braun, J.: HyLands 1.0: a Hybrid Landscape
1095 evolution model to simulate the impact of landslides and landslide-derived sediment on landscape evolution, Geoscientific Model Development, 13, 3863–3886, 2020.

Ceriani, M., Lauzi, S., and Padovan, M.: Rainfall thresholds triggering debris-flow in the alpine area of Lombardia Region, central Alps – Italy, in: In Proceedings of the Man and Mountain'94, First International Congress for the Protection and Development of Mountain Environmen, Ponte di Legno (BS), Italy, 1994.

1100 Cevasco, A., Pepe, G., and Brandolini, P.: The influences of geological and land use settings on shallow landslides triggered by an intense rainfall event in a coastal terraced environment, Bulletin of Engineering Geology and the Environment, 73, 859–875, https://doi.org/10.1007/s10064-013-0544-x, 2014.

Chen, L. and Young, M. H.: Green-Ampt infiltration model for sloping surfaces, Water Resources Research, 42, https://doi.org/10.1029/2005WR004468, 2006.

1105 Chow, V. T., Maidment, D. R., and Mays, L. W.: Applied hydrology, McGraw-Hill, New York, 1988.

Ciccarese, G., Mulas, M., Alberoni, P. P., Truffelli, G., and Corsini, A.: Debris flows rainfall thresholds in the Apennines of Emilia-Romagna (Italy) derived by the analysis of recent severe rainstorms events and regional meteorological data, Geomorphology, 358, 107097, https://doi.org/10.1016/j.geomorph.2020.107097, 2020.

Cislaghi, A., Chiaradia, E. A., and Bischetti, G. B.: Including root reinforcement variability in a probabilistic 3D
stability model, Earth Surface Processes and Landforms, 42, 1789–1806, https://doi.org/10.1002/esp.4127, 2017.

CNR and IRPI: Rapporto Periodico sul Rischio posto alla Popolazione italiana da Frane e Inondazioni, Anno 2020,
19 pp., https://doi.org/10.30437/report2020, 2021.

Collischonn, W., Fleischmann, A., Paiva, R. C. D., and Mejia, A.: Hydraulic Causes for Basin Hydrograph
Skewness, Water Resources Research, 53, 10603–10618, https://doi.org/10.1002/2017WR021543, 2017.

Crosta, G. B. and Frattini, P.: Distributed modelling of shallow landslides triggered by intense rainfall, Natural
Hazards and Earth System Sciences, 3, 81–93, https://doi.org/10.5194/nhess-3-81-2003, 2003.

Crosta, G. B., Imposimato, S., and Roddeman, D. G.: Numerical modelling of large landslides stability and runout,
Nat. Hazards Earth Syst. Sci., 3, 523–538, https://doi.org/10.5194/nhess-3-523-2003, 2003.

Dade, W. B. and Friend, P. F.: Grain-Size, Sediment-Transport Regime, and Channel Slope in Alluvial Rivers, The
Journal of Geology, 106, 661–676, https://doi.org/10.1086/516052, 1998.

Daly, C., Slater, M. E., Roberti, J. A., Laseter, S. H., and Swift Jr, L. W.: High-resolution precipitation mapping in
a mountainous watershed: ground truth for evaluating uncertainty in a national precipitation dataset, International
Journal of Climatology, 37, 124–137, https://doi.org/10.1002/joc.4986, 2017.

D'Amato Avanzi, G., Giannecchini, R., and Puccinelli, A.: The influence of the geological and geomorphological
settings on shallow landslides. An example in a temperate climate environment: the June 19, 1996 event in
northwestern Tuscany (Italy), Engineering Geology, 73, 215–228, https://doi.org/10.1016/j.enggeo.2004.01.005,
2004.

Dapporto, S., Aleotti, P., Casagli, N., and Polloni, G.: Analysis of shallow failures triggered by the 14-16 November
2002 event in the Albaredo valley, Valtellina (Northern Italy), Advances in Geosciences, 2, 305–308,
https://doi.org/10.5194/adgeo-2-305-2005, 2005.

De Vita, P., Fusco, F., Tufano, R., and Cusano, D.: Seasonal and Event-Based Hydrological and Slope Stability
Modeling of Pyroclastic Fall Deposits Covering Slopes in Campania (Southern Italy), Water, 10, 1140,
https://doi.org/10.3390/w10091140, 2018.

Devia, G. K., Ganasri, B. P., and Dwarakish, G. S.: A Review on Hydrological Models, Aquatic Procedia, 4, 1001–
1007, https://doi.org/10.1016/j.aqpro.2015.02.126, 2015.

Fan, Y., Miguez-Macho, G., Weaver, C. P., Walko, R., and Robock, A.: Incorporating water table dynamics in
climate modeling: 1. Water table observations and equilibrium water table simulations, Journal of Geophysical
Research: Atmospheres, 112, https://doi.org/10.1029/2006JD008111, 2007.

Fawcett, T.: An introduction to ROC analysis, Pattern Recognition Letters, 27, 861–874,
https://doi.org/10.1016/j.patrec.2005.10.010, 2006.

Formetta, G., Capparelli, G., and Versace, P.: Evaluating performance of simplified physically based models for shallow landslide susceptibility, Hydrology and Earth System Sciences, 20, 4585–4603, https://doi.org/10.5194/hess-20-4585-2016, 2016.

G., C., M., M., and A., C.: Combining spatial modelling and regionalization of rainfall thresholds for debris flows hazard mapping in the Emilia-Romagna Apennines (Italy), Landslides, 18, 3513–3529, https://doi.org/10.1007/s10346-021-01739-w, 2021.

Gao, L., Zhang, L. M., and Cheung, R. W. M.: Relationships between natural terrain landslide magnitudes and triggering rainfall based on a large landslide inventory in Hong Kong, Landslides, 15, 727–740, https://doi.org/10.1007/s10346-017-0904-x, 2018.

Gariano, S. L. and Guzzetti, F.: Landslides in a changing climate, Earth-Science Reviews, 162, 227–252, https://doi.org/10.1016/j.earscirev.2016.08.011, 2016.

GDAL/OGR contributors: GDAL/OGR Geospatial Data Abstraction software Library, Open Source Geospatial Foundation, 2020.

Girard, M.-C., Girard, C., Dominique, C., Gilliot, J.-M., Loubersac, L., Meyer-Roux, J., Monget, J.-M., Seguin, B., and Rao, N.: Corine Land Cover, 331–344, https://doi.org/10.1201/9780203741917-19, 2018.

Gleick, P. H.: Climate change, hydrology, and water resources, Reviews of Geophysics, 27, 329–344, https://doi.org/10.1029/RG027i003p00329, 1989.

Globevnik, L., Holjevj_, D., Petkowaek, G., and Rubinj_, J.: 145. Applicability of the Gavrilo vic Method in Erosion Calculation Using Spatial Data Manipulation Techniques, Tunnelling and Underground Space Technology, 14, 2003.

Govers, G.: Empirical relationships for the transport capacity of overland flow., 1989.

Govers, G., Wallings, D. E., Yair, A., and Berkowicz, S.: Empirical relationships for the transport capacity of overland flow, International Association of Hydrological Sciences, 189, 1990.

de Graaf, I. E. M., Sutanudjaja, E. H., van Beek, L. P. H., and Bierkens, M. F. P.: A high-resolution global-scale groundwater model, Hydrol. Earth Syst. Sci., 19, 823–837, https://doi.org/10.5194/hess-19-823-2015, 2015.

Groenendyk, D. G., Ferré, T. P. A., Thorp, K. R., and Rice, A. K.: Hydrologic-Process-Based Soil Texture Classifications for Improved Visualization of Landscape Function., PLoS One, 10, e0131299, https://doi.org/10.1371/journal.pone.0131299, 2015.

Gudiyangada Nachappa, T., Tavakkoli Piralilou, S., Ghorbanzadeh, O., Shahabi, H., and Blaschke, T.: Landslide Susceptibility Mapping for Austria Using Geons and Optimization with the Dempster-Shafer Theory, Applied Sciences, 9, https://doi.org/10.3390/app9245393, 2019.

Guzzetti, F., Reichenbach, P., Cardinali, M., Galli, M., and Ardizzone, F.: Probabilistic landslide hazard assessment at the basin scale, Geomorphology, 72, 272–299, https://doi.org/10.1016/j.geomorph.2005.06.002, 2005.

Guzzetti, F., Peruccacci, S., Rossi, M., and Stark, C. P.: Rainfall thresholds for the initiation of landslides in central
1175 and southern Europe, Meteorology and Atmospheric Physics, 98, 239–267, https://doi.org/10.1007/s00703-007-
0262-7, 2007.

Harp, E. L., Michael, J. A., and Laprade, W. T.: Shallow-landslide hazard map of Seattle, Washington, Reston,
VA, https://doi.org/10.3133/ofr20061139, 2006.

Hayashi, M.: Alpine Hydrogeology: The Critical Role of Groundwater in Sourcing the Headwaters of the World,
1180 Groundwater, 58, 498–510, https://doi.org/10.1111/gwat.12965, 2020.

Hengl, T., Mendes de Jesus, J., Heuvelink, G. B. M., Ruiperez Gonzalez, M., Kilibarda, M., Blagotić, A.,
Shangguan, W., Wright, M. N., Geng, X., Bauer-Marschallinger, B., Guevara, M. A., Vargas, R., MacMillan, R.
A., Batjes, N. H., Leenaars, J. G. B., Ribeiro, E., Wheeler, I., Mantel, S., and Kempen, B.: SoilGrids250m: Global
gridded soil information based on machine learning, PLOS ONE, 12, e0169748,
1185 https://doi.org/10.1371/journal.pone.0169748, 2017.

Herrera, M.: Landslide Detection using Random Forest Classifier, https://doi.org/10.13140/RG.2.2.31365.91369,
2019.

Hungr, O., McDougall, S., Wise, M., and Cullen, M.: Magnitude–frequency relationships of debris flows and debris
avalanches in relation to slope relief, Geomorphology, 96, 355–365,
1190 https://doi.org/10.1016/j.geomorph.2007.03.020, 2008.

Huscroft, J., Gleeson, T., Hartmann, J., and Börker, J.: Compiling and Mapping Global Permeability of the
Unconsolidated and Consolidated Earth: GLobal HYdrogeology MaPS 2.0 (GLHYMPS 2.0), Geophysical
Research Letters, 45, https://doi.org/10.1002/2017GL075860, 2018.

Inventario Fenomeni Franosi: http://www.isprambiente.gov.it/it/progetti/suolo-e-territorio-1/iffi-inventario-dei-
1195 fenomeni-franosi-in-italia.

ISPRA: Dissesto idrogeologico in Italia: pericolosità e indicatori di rischio, ISPRA, Ispra, 2018.

ITCOLD: La gestione dell'interrimento dei serbatoi artificiali italiani, Comitato Nazionale Italiano delle Grandi
Dighe, 2009.

ITCOLD: La gestione dell'interrimento dei serbatoi artificiali italiani situazione attuale e prospettive, Comitato
1200 Nazionale Italiano delle Grandi Dighe, 2016.

Ivanov, V., Radice, A., Papini, M., and Longoni, L.: Event-scale pebble mobility observed by RFID tracking in a
pre-Alpine stream: a field laboratory, Earth Surface Processes and Landforms, 45, 535–547,
https://doi.org/10.1002/esp.4752, 2020a.

Ivanov, V., Arosio, D., Tresoldi, G., Hojat, A., Zanzi, L., Papini, M., and Longoni, L.: Investigation on the Role of
1205 Water for the Stability of Shallow Landslides-Insights from Experimental Tests, Water, 12(4), 2020b.

Iverson, R., Reid, M., and Lahusen, R.: Debris-flow mobilization from landslides. Annu Rev Earth Planet Sci, Annu. Rev. Earth Planet. Sci, 25, 85–138, https://doi.org/10.1146/annurev.earth.25.1.85, 1997.

Iverson, R. M.: Landslide triggering by rain infiltration, Water Resources Research, 36, 1897–1910, https://doi.org/10.1029/2000WR900090, 2000.

1210 Jackson, C. R., Bitew, M., and Du, E.: When interflow also percolates: downslope travel distances and hillslope process zones, Hydrological Processes, 28, 3195–3200, https://doi.org/10.1002/hyp.10158, 2014.

Jakob, M. and Jordan, P.: Design flood estimates in mountain streams – the need for a geomorphic approach, Can. J. Civ. Eng., 28, 425–439, https://doi.org/10.1139/l01-010, 2001.

Jie, T., Zhang, B., He, C., and Yang, L.: Variability In Soil Hydraulic Conductivity And Soil Hydrological
1215 Response Under Different Land Covers In The Mountainous Area Of The Heihe River Watershed, Northwest China, Land Degradation & Development, 28, https://doi.org/10.1002/ldr.2665, 2016.

Kadavi, P., Lee, C.-W., and Lee, S.: Application of Ensemble-Based Machine Learning Models to Landslide Susceptibility Mapping, Remote Sensing, 10, 1252, https://doi.org/10.3390/rs10081252, 2018.

Karssenberg, D., Schmitz, O., Salamon, P., de Jong, K., and Bierkens, M. F. P.: A software framework for
1220 construction of process-based stochastic spatio-temporal models and data assimilation, Environmental Modelling & Software, 25, 489–502, https://doi.org/10.1016/j.envsoft.2009.10.004, 2010.

Kim, K.-S., Kim, M.-I., Lee, M.-S., and Hwang, E.-S.: Regression Equations for Estimating Landslide-Triggering Factors Using Soil Characteristics, Applied Sciences, 10, https://doi.org/10.3390/app10103560, 2020.

Klaus, J. and Jackson, C. R.: Interflow Is Not Binary: A Continuous Shallow Perched Layer Does Not Imply
1225 Continuous Connectivity, Water Resources Research, 54, 5921–5932, https://doi.org/10.1029/2018WR022920, 2018.

Kobierska, F., Jonas, T., Kirchner, J. W., and Bernasconi, S. M.: Linking baseflow separation and groundwater storage dynamics in an alpine basin (Dammagletscher, Switzerland), Hydrol. Earth Syst. Sci., 19, 3681–3693, https://doi.org/10.5194/hess-19-3681-2015, 2015.

1230 Kondolf, george 'mathias: Hungry Water: Effects of Dams and Gravel Mining on River Channels, Environmental Management, 21, 533–551, https://doi.org/10.1007/s002679900048, 1997.

Lamb, M. P. and Venditti, J. G.: The grain size gap and abrupt gravel-sand transitions in rivers due to suspension fallout, Geophysical Research Letters, 43, 3777–3785, https://doi.org/10.1002/2016GL068713, 2016.

Langland, M. J.: Bathymetry and Sediment-Storage Capacity Change in Three Reservoirs on the Lower
1235 Susquehanna River, 1996-2008, https://doi.org/10.3133/sir20095110, 2009.

Lazzari, M., Piccarreta, M., and Manfreda, S.: The role of antecedent soil moisture conditions on rainfall-triggered shallow landslides, Natural Hazards and Earth System Sciences Discussions, 2018, 1–11, https://doi.org/10.5194/nhess-2018-371, 2018.

Lee, K. and Pin Chun, H.: Evaluating the adequateness of kinematic-wave routing for flood forecasting in
1240 midstream channel reaches of Taiwan, Journal of Hydroinformatics, 14, 1075,
https://doi.org/10.2166/hydro.2012.093, 2012.

Lehner, B., Verdin, K., and Jarvis, A.: New Global Hydrography Derived From Spaceborne Elevation Data, Eos,
Transactions American Geophysical Union, 89, 93–94, https://doi.org/10.1029/2008EO100001, 2008.

Longoni, L., Ivanov, V. I., Brambilla, D., Radice, A., and Papini, M.: Analysis of the temporal and spatial scales
1245 of soil erosion and transport in a Mountain Basin, Italian Journal of Engineering Geology and Environment, 16,
17–30, https://doi.org/10.4408/IJEGE.2016-02.O-02, 2016.

Ly, S., Charles, C., and Degre, A.: Different methods for spatial interpolation of rainfall data for operational
hydrology and hydrological modeling at watershed scale. A review, Biotechnology, Agronomy and Society and
Environment, 17, 392–406, 2013.

1250 Mandal, S. and Maiti, R.: Impact Assessment of Hydrologic Attributes and Slope Instability, in: Semi-quantitative
Approaches for Landslide Assessment and Prediction, edited by: Mandal, S. and Maiti, R., Springer Singapore,
Singapore, 95–121, https://doi.org/10.1007/978-981-287-146-6_3, 2015.

Marnezy, A.: Alpine dams. From hydroelectric power to artificial snow, Revue de géographie alpine, 96, 2008.

Meisina, C., Zizioli, D., and Zucca, F.: Methods for Shallow Landslides Susceptibility Mapping: An Example in
1255 Oltrepo Pavese, 1, 451–457, https://doi.org/10.1007/978-3-642-31325-7-58, 2013.

Merritt, W. S., Letcher, R. A., and Jakeman, A. J.: A review of erosion and sediment transport models,
Environmental Modelling & Software, 18, 761–799, https://doi.org/10.1016/S1364-8152(03)00078-1, 2003.

Milanesi, L., Pilotti, M., Clerici, A., and Gavrilovic, Z.: Application of an improved version of the Erosion Potential
Method in Alpine areas, Italian Journal of Engineering Geology and Environment,
1260 https://doi.org/10.4408/IJEGE.2015-01.O-02, 2015.

Milledge, D. G., Bellugi, D., McKean, J. A., Densmore, A. L., and Dietrich, W. E.: A multidimensional stability
model for predicting shallow landslide size and shape across landscapes, Journal of Geophysical Research: Earth
Surface, 119, 2481–2504, https://doi.org/10.1002/2014JF003135, 2014.

Mishra, S. K., Tyagi, J. V., and Singh, V. P.: Comparison of infiltration models, Hydrological Processes, 17, 2629–
1265 2652, https://doi.org/10.1002/hyp.1257, 2003.

Moges, E., Demissie, Y., Larsen, L., and Yassin, F.: Review: Sources of Hydrological Model Uncertainties and
Advances in Their Analysis, Water, 13, https://doi.org/10.3390/w13010028, 2021.

Montgomery, D. R. and Dietrich, W. E.: A physically based model for the topographic control on shallow
landsliding, Water Resources Research, 30, 1153–1171, https://doi.org/10.1029/93WR02979, 1994.

1270 Montrasio, L.: Stability of soil-slip, Wit Press, Risk Analysis II, 45, 357–366, https://doi.org/10.2495/RISK000331,
2008.

Montrasio, L. and Valentino, R.: Modelling Rainfall-induced Shallow Landslides at Different Scales Using SLIP - Part II, Procedia Engineering, 158, 482–486, https://doi.org/10.1016/j.proeng.2016.08.476, 2016.

Morbidelli, R., Corradini, C., Saltalippi, C., Flammini, A., Dari, J., and Govindaraju, R. S.: Rainfall Infiltration Modeling: A Review, Water, 10, https://doi.org/10.3390/w10121873, 2018.

Morgan, R. P. C. and Nearing, M. A.: Handbook of erosion modelling., 2011.

Mostbauer, K., Kaitna, R., Prenner, D., and Hrachowitz, M.: The temporally varying roles of rainfall, snowmelt and soil moisture for debris flow initiation in a snow-dominated system, Hydrol. Earth Syst. Sci., 22, 3493–3513, https://doi.org/10.5194/hess-22-3493-2018, 2018.

Munich Re: Natural disasters caused overall losses of US $ 210bn Relevant natural catastrophe loss events worldwide 2020, 1, 2021.

Nino, Y.: Simple Model for Downstream Variation of Median Sediment Size in Chilean Rivers, Journal of Hydraulic Engineering, 128, 934–941, 2002.

Pacina, J., Lenďáková, Z., Štojdl, J., Matys Grygar, T., and Dolejš, M.: Dynamics of Sediments in Reservoir Inflows: A Case Study of the Skalka and Nechranice Reservoirs, Czech Republic, ISPRS International Journal of Geo-Information, 9, https://doi.org/10.3390/ijgi9040258, 2020.

Papini, M., Ivanov, V., Brambilla, D., Arosio, D., and Longoni, L.: Monitoring bedload sediment transport in a pre-Alpine river: An experimental method, Rendiconti Online della Società Geologica Italiana, 43, 57–63, https://doi.org/10.3301/ROL.2017.35, 2017.

Pearson, E., Smith, M. W., Klaar, M. J., and Brown, L. E.: Can high resolution 3D topographic surveys provide reliable grain size estimates in gravel bed rivers?, Geomorphology, 293, 143–155, https://doi.org/10.1016/j.geomorph.2017.05.015, 2017.

Pebesma, E. J., de Jong, K., and Briggs, D.: Interactive visualization of uncertain spatial and spatio-temporal data under different scenarios: an air quality example, null, 21, 515–527, https://doi.org/10.1080/13658810601064009, 2007.

Peirce, S., Ashmore, P., and Leduc, P.: Evolution of grain size distributions and bed mobility during hydrographs in gravel-bed braided rivers, Earth Surface Processes and Landforms, 44, 304–316, https://doi.org/10.1002/esp.4511, 2019.

Pelletier, J. D., Broxton, P. D., Hazenberg, P., Zeng, X., Troch, P. A., Niu, G.-Y., Williams, Z., Brunke, M. A., and Gochis, D.: A gridded global data set of soil, intact regolith, and sedimentary deposit thicknesses for regional and global land surface modeling, Journal of Advances in Modeling Earth Systems, 8, 41–65, https://doi.org/10.1002/2015MS000526, 2016.

Pereira, S., Garcia, R., Zêzere, J., Oliveira, S., and Silva, M.: Landslide quantitative risk analysis of buildings at the municipal scale based on a rainfall triggering scenario, Geomatics, Natural Hazards and Risk, 8, https://doi.org/10.1080/19475705.2016.1250116, 2016.

Rahardjo, H., Satyanaga, A., Leong, E. C., Santoso, V. A., and Ng, Y. S.: Performance of an instrumented slope covered with shrubs and deep-rooted grass, Soils and Foundations, 54, 417–425, https://doi.org/10.1016/j.sandf.2014.04.010, 2014.

Ravi, V., Williams, J. R., and Ouyang, Y.: Estimation of infiltration rate in the vadose zone: compilation of simple mathematical models, 1998.

Raziei, T. and Pereira, L.: Estimation of ETo with Hargreaves-Samani and FAO-PM temperature methods for a wide range of climates in Iran, Agricultural Water Management, 121, 1–18, https://doi.org/10.1016/j.agwat.2012.12.019, 2013.

Remondo, J., Bonachea, J., and Cendrero, A.: A statistical approach to landslide risk modelling at basin scale: From landslide susceptibility to quantitative risk assessment, Landslides, 2, 321–328, https://doi.org/10.1007/s10346-005-0016-x, 2005.

Rickenmann, D.: Empirical Relationships for Debris Flows, Natural Hazards, 19, 47–77, https://doi.org/10.1023/A:1008064220727, 1999.

Ronchetti, F., Borgatti, L., Cervi, F., C, G., Piccinini, L., Vincenzi, V., and Alessandro, C.: Groundwater processes in a complex landslide, northern Apennines, Italy, Natural Hazards and Earth System Sciences, 9, 895–904, https://doi.org/10.5194/nhess-9-895-2009, 2009.

Roo, A., A.P.J, Wesseling, C. G., Jetten, V. G., and Ritsema, C.: LISEM: A physically-based hydrological and soil erosion model incorporated in a GIS, In: K. Kovar & H.P. Nachtnebel (eds.), Application of geographic information systems in hydrology and water resources management. Wallingford (UK), IAHS, 1996. IAHS Publ. 235, pp. 395-403, 1996.

Ross, C. W., Prihodko, L., Anchang, J., Kumar, S., Ji, W., and Hanan, N. P.: HYSOGs250m, global gridded hydrologic soil groups for curve-number-based runoff modeling, Sci Data, 5, 180091–180091, https://doi.org/10.1038/sdata.2018.91, 2018.

Sambrook Smith, G. H. and Ferguson, R. I.: The gravel-sand transition along river channels, Journal of Sedimentary Research, 65, 423–430, https://doi.org/10.1306/D42680E0-2B26-11D7-8648000102C1865D, 1995.

Scheidl, C. and Rickenmann, D.: TopFlowDF - A simple gis based model to simulate debris-flow runout on the fan, https://doi.org/10.4408/IJEGE.2011-03.B-030, 2011.

Schellekens, J., Verseveld, W. van, Visser, M., hcwinsemius, laurenebouaziz, tanjaeuser, sandercdevries, cthiange, hboisgon, DirkEilander, DanielTollenaar, aweerts, Baart, F., Pieter9011, Pronk, M., arthur-lutz, ctenvelden, Imme1992, and Jansen, M.: openstreams/wflow: Bug fixes and updates for release 2020.1.2, Zenodo, https://doi.org/10.5281/zenodo.4291730, 2020.

Shobe, C., Tucker, G., and Barnhart, K.: The SPACE 1.0 model: A Landlab component for 2-D calculation of sediment transport, bedrock erosion, and landscape evolution, Geoscientific Model Development Discussions, 1–38, https://doi.org/10.5194/gmd-2017-175, 2017.

1340   Smith, R. E. and Parlange, J.-Y.: A parameter-efficient hydrologic infiltration model, Water Resources Research, 14, 533–538, https://doi.org/10.1029/WR014i003p00533, 1978.

Strauch, R., Istanbulluoglu, E., Nudurupati, S. S., Bandaragoda, C., Gasparini, N. M., and Tucker, G. E.: A hydroclimatological approach to predicting regional landslide probability using Landlab, Earth Surf. Dynam., 6, 49–75, https://doi.org/10.5194/esurf-6-49-2018, 2018.

1345   Sutanudjaja, E. H., van Beek, R., Wanders, N., Wada, Y., Bosmans, J. H. C., Drost, N., van der Ent, R. J., de Graaf, I. E. M., Hoch, J. M., de Jong, K., Karssenberg, D., López López, P., Peßenteiner, S., Schmitz, O., Straatsma, M. W., Vannametee, E., Wisser, D., and Bierkens, M. F. P.: PCR-GLOBWB 2: a 5\,arcmin global hydrological and water resources model, Geoscientific Model Development, 11, 2429–2453, https://doi.org/10.5194/gmd-11-2429-2018, 2018.

1350   Takahashi, T.: A Review of Japanese Debris Flow Research, International Journal of Erosion Control Engineering, 2, https://doi.org/10.13101/ijece.2.1, 2009.

Tangi, M., Schmitt, R., Bizzi, S., and Castelletti, A.: The CASCADE toolbox for analyzing river sediment connectivity and management, Environmental Modelling & Software, 119, 400–406, https://doi.org/10.1016/j.envsoft.2019.07.008, 2019.

1355   Theule, J.: Geomorphic study of sediment dynamics in active debris-flow catchments (French Alps), 2012.

Tóth, B., Weynants, M., Pásztor, L., and Hengl, T.: 3D soil hydraulic database of Europe at 250 m resolution, Hydrological Processes, 31, 2662–2666, https://doi.org/10.1002/hyp.11203, 2017.

Tramblay, Y., Bouvier, C., Martin, C., Didon-Lescot, J.-F., Todorovik, D., and Domergue, J.-M.: Assessment of initial soil moisture conditions for event-based rainfall–runoff modelling, Journal of Hydrology, 387, 176–187, 1360   https://doi.org/10.1016/j.jhydrol.2010.04.006, 2010.

Uber, M., Vandervaere, J.-P., Zin, I., Braud, I., Heistermann, M., Legoût, C., Molinié, G., and Nord, G.: How does initial soil moisture influence the hydrological response? A case study from southern France, Hydrology and Earth System Sciences, 22, 6127–6146, https://doi.org/10.5194/hess-22-6127-2018, 2018.

Vakhshoori, V. and Zare, M.: Is the ROC curve a reliable tool to compare the validity of landslide susceptibility 1365   maps?, null, 9, 249–266, https://doi.org/10.1080/19475705.2018.1424043, 2018.

Van Der Knijff, J. M., Younis, J., and De Roo, A. P. J.: LISFLOOD: a GIS-based distributed model for river basin scale water balance and flood simulation, null, 24, 189–212, https://doi.org/10.1080/13658810802549154, 2010.

Van Genuchten, M.: A Closed-form Equation for Predicting the Hydraulic Conductivity of Unsaturated Soils1, Soil Science Society of America Journal, 44, https://doi.org/10.2136/sssaj1980.03615995004400050002x, 1980.

1370   Vardon, P. J., Liu, K., and Hicks, M. A.: Reduction of slope stability uncertainty based on hydraulic measurement via inverse analysis, null, 10, 223–240, https://doi.org/10.1080/17499518.2016.1180400, 2016.

de Vente, J. and Poesen, J.: Predicting soil erosion and sediment yield at the basin scale: Scale issues and semi-quantitative models, Earth-Science Reviews, 71, 95–125, https://doi.org/10.1016/j.earscirev.2005.02.002, 2005.

Vetsch, D., Siviglia, A., Caponi, F., Ehrbar, D., Gerke, E., Kammerer, S., Koch, A., Peter, S., Vanzo, D., Vonwiller, L., Facchini, M., Gerber, M., Volz, C., Farshi, D., Mueller, R., Rousselot, P., Veprek, R., and Faeh, R.: System Manuals of BASEMENT Version 2.8, 2018.

Vitvar, T., Burns, D. A., Lawrence, G. B., McDonnell, J. J., and Wolock, D. M.: Estimation of baseflow residence times in watersheds from the runoff hydrograph recession: method and application in the Neversink watershed, Catskill Mountains, New York, Hydrological Processes, 16, 1871–1877, https://doi.org/10.1002/hyp.5027, 2002.

Yu, B., Xie, C., Cai, S., Chen, Y., Lv, Y., Mo, Z., Liu, T., and Yang, Z.: Effects of Tree Root Density on Soil Total Porosity and Non-Capillary Porosity Using a Ground-Penetrating Tree Radar Unit in Shanghai, China, Sustainability, 10, https://doi.org/10.3390/su10124640, 2018.

Zhu, Y. and Xiao, Y.: Slope Stability from a Hydrological Perspective: Taking Typical Soil Slope as an Example, Advances in Civil Engineering, 2020, 1273603, https://doi.org/10.1155/2020/1273603, 2020.

Zomlot, Z., Verbeiren, B., Huysmans, M., and Batelaan, O.: Spatial distribution of groundwater recharge and base flow: Assessment of controlling factors, Journal of Hydrology: Regional Studies, 4, 349–368, https://doi.org/10.1016/j.ejrh.2015.07.005, 2015.